Structures 63 (2024) 106408

Contents lists available at ScienceDirect

Structures

journal homepage: www.elsevier.com/locate/structures

Seismic assessment of a dome structure with minarets as secondary elements: The case of Soltaniyeh Dome in Iran

Arezu Feizolahbeigi *, Rafael Ramirez, Paulo B. Lourenço

ISISE, Department of Civil Engineering, University of Minho, Campus de Azurem, 4800-058, Guimarães, Portugal

A R T I C L E I N F O

Keywords:
Soltaniyeh Dome
Seismic assessment
Pushover analysis
Box dome
Minaret
Iranian architecture

A B S T R A C T

The Soltaniyeh Dome, located in Iran, was built in the 14th century as a mausoleum. The building possesses several distinctive features that categorize it as a unique masterpiece of Iranian architecture. Notably, the double-shell dome of the structure represents a particular dome construction technique, in which the two parallel shells are connected through a network of ribs. This research aims to assess the seismic performance of the dome and its surrounding minarets as secondary elements. The methodology of this work starts with a historical survey of the building and its context followed by a review of the state of the art, preparation, and calibration of three-dimensional numerical models according to the defined scenarios, and performing seismic analysis including pushover analysis and limit analysis to assess the seismic behavior of the entire structure. The results from seismic analyses provide the collapse mechanisms of the entire structure. Additionally, minarets were identified as the most vulnerable part of the structure.

1. Introduction

Iranian domes have an ancient origin and a rich history extending to the modern era. The use of the domes in ancient Mesopotamia was carried forward through a succession of empires in the Greater Iran region [1]. Domes became an integral part of buildings due to the scarcity of wood in many areas of the Iranian plateau [2] and were at the forefront of Iranian architecture during the Sasanid period (224–651 A.D.). They evolved through different eras until the Safavid era (1501–1732 A.D.) when the last generation of Iranian domes was characterized by a distinctive bulbous profile and astonishing tilework [3]. Depending on the importance of the domed building, different visual characteristics, including dimensions and additional elements such as minarets and decorations, were defined or added to the structure. Minaret in Iranian architecture is often found at the entrance of religious areas like mosques and tombs, positioned symmetrically on both sides of the *Ivan* (porch), or as isolated watchtowers known as *Mil*. However, there is a unique domed structure called Soltaniyeh Dome (*Gonbade Soltaniyeh)* (1302–1312 A.D.) that exhibits several distinctive features: a massive structure with a double-shell box dome connected by a network of ribs, parallel shells, and eight tall minarets surrounding the dome. Its architectural style has inspired the construction of other dome structures [4]. Exploring Iranian architectural culture through the study of different structural types and forms reveals a deliberate approach to the construction of both structural and nonstructural elements in buildings, which can be considered secondary structure elements. Prominent structural elements in Iranian architecture are the second and third shells in the domes and minarets. In the case of the Soltaniyeh Dome, minarets are considered secondary structure elements.

Masonry domes in heritage structures are highly vulnerable to earthquakes due to their low tensile strength and degradation. Therefore, in seismically active regions, one of the most important issues concerning masonry domes is the study of their seismic behavior, especially when additional structural elements might affect their response. Preserving cultural and historical structures, especially in seismic-prone areas is of utmost importance. For this reason, several experimental and theoretical studies have been performed to improve analysis methods and assessment tools, aiming to mitigate the seismic vulnerability of such structures. The review of literature on the structural investigation of masonry domes and minarets provides valuable insights into the topic, indicating the application of a wide range of classical to modern methods. Several scholars have investigated the behavior of such structures under static and dynamic loads by theoretical formulations and structural analysis methods discussing potential failure mechanisms [5–20]. In most of these studies the use of numerical analysis based on the finite element method is prominent. This method is

* Corresponding author.
E-mail address: a.feizolahbeigi@ut.ac.ir (A. Feizolahbeigi).

https://doi.org/10.1016/j.istruc.2024.106408
Received 20 November 2023; Received in revised form 10 March 2024; Accepted 10 April 2024
Available online 16 April 2024

(a) (b)

Fig. 1. Citadel and the archeological site of Soltaniyeh [60].

a powerful tool for understanding the structural behavior of masonry constructions, [16,21–24] and has been extensively and successfully employed in the numerical analysis of masonry constructions. Although the application of the finite element method faces certain limitations, such as challenges in obtaining precise mechanical properties and the variety of input parameters required for the models [25,26] a combination of numerical methods and empirical observations proves beneficial [27]. This approach has been used in various studies to assess the safety and structural performance of dome structures after structural interventions [28–36], while also highlighting the challenges and advancements in preserving and retrofitting these structures [37,38]. Additionally, dedicated literature is focused on the effect of geometry and construction techniques on the structural response of the dome structures [16,25,27,39–42].

Considering the case of the Soltaniyeh Dome, which is the focus of this study, it is essential to investigate the seismic performance of the structure given its location in a high seismic prone zone. Hence, the structural function and seismic behavior of the dome and minarets have been extensively discussed and investigated by numerous scholars [43–47].

In these studies, the response of the structure to the various real earthquake loads has been evaluated, identifying vulnerable parts of the structure.

In the aforementioned studies, the utilized models often fail to accurately represent the actual situation of the structure, as they frequently omit crucial elements such as openings, the tomb and other structural elements that significantly affect the overall structural response of the building. Additionally, the structural interventions are usually not included in these models. While simplified partial models may be suitable in certain instances, a comprehensive global model proves more effective in capturing the seismic response of the structure [47]. On the contrary, the 3D model used in the present study is a much more accurate representation derived from precise measurement of the entire structure. It encompasses the real configuration of the structure, including the alterations, interventions and deformations that have occurred throughout its lifespan.

Another type of analysis, which offers a more practical approach for estimating the maximum load capacity of the structure with a reduced number of parameters is the limit analysis. This approach involves considering the structure as a combination of macro-blocks [20,48–53]. The limit analysis method, commonly used by other scholars [52, 54–59], has also been employed in this study.

This research aims to investigate the seismic behavior of the Soltaniyeh Dome, with emphasis on its minarets and their structural function in case of an earthquake. In general, the present work has two contributions. First, it provides a further understanding of the structural behavior of massive dome structures and, second, it addresses the effects of secondary structural components.

In order to accomplish the objectives of the study, a concise literature review was initially conducted, followed by an exploration of the geographical context in which the mausoleum is located. This exploration included considerations of morphology, hydrology, climate, and seismic activity specific to the region. Subsequently, a historical survey was performed to obtain information about the main characteristics of the building, including geometry, design, decorations, and construction techniques. This was complemented by documentation of previous interventions and restoration works. Moreover, the current state of the mausoleum was assessed involving in-situ visual inspections and damage surveys of both the exterior and the interior of the building. Based on the previously collected geometric and material data, three different 3D finite element models of the mausoleum were prepared. These models corresponded to three different scenarios defined for the mausoleum, namely the original configuration, the original configuration without minarets, and the present-day configuration.

The seismic performance of the mausoleum was investigated by performing pushover analyses in three different configurations, together with limit analysis for four different collapse mechanisms based on macroblocks. Finally, the results of these analyses were discussed and compared to justify the current condition of the structure and assess its safety. Conclusions were subsequently provided.

2. Description of the Soltaniyeh Dome

The Soltaniyeh Dome is located in the northwestern city of Soltaniyeh, which briefly served as the capital of the Ilkhanid dynasty during the 13th and 14th centuries. The building was constructed as the mausoleum for the king Oljaytu. The mausoleum was covered by a massive brick dome, which soon gave its name to the whole building, "Soltaniyeh Dome". The surrounding area of the Soltaniyeh Dome encompasses a stone terrace in the form of a citadel, covering an area of 18 ha. Archaeological excavations revealed the remains of the citadel, comprising a stone platform with 16 towers and a gate (Fig. 1a). The mausoleum includes a magnificent dome covered with turquoise-blue faience tiles, along with the tomb and a cellar (Fig. 1b). In the urban landscape, the dome emerges as a vibrant burst of color, immediately capturing attention. The eight minarets that surround the dome become the next focal point for the observer. Soltaniyeh Dome is recognized as the architectural masterpiece of its time and an outstanding achievement in the development of Persian architecture, particularly in its innovative double-shelled dome and interior decoration.

The mausoleum dome's double-shell structure and the materials and themes used for its interior decoration are of special relevance. The

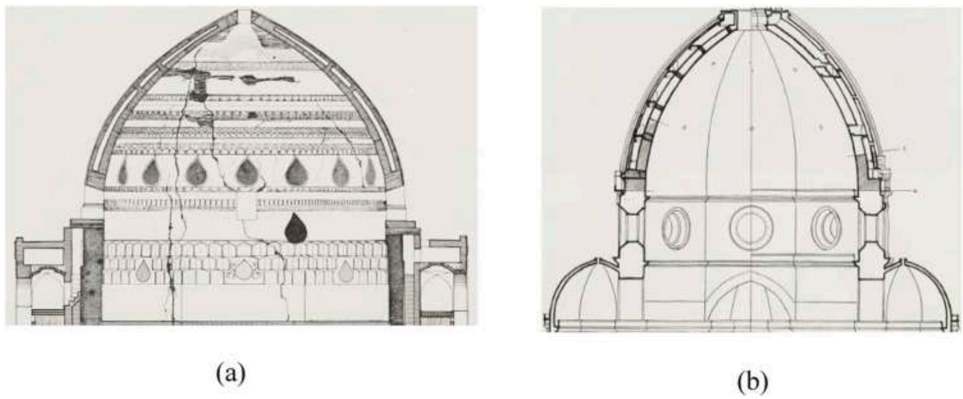

Fig. 2. Architectural configuration: (a) Dome of Soltaniyeh; (b) Dome of Santa Maria in Florence, Italy [4] (Sketches are not on the same scale).

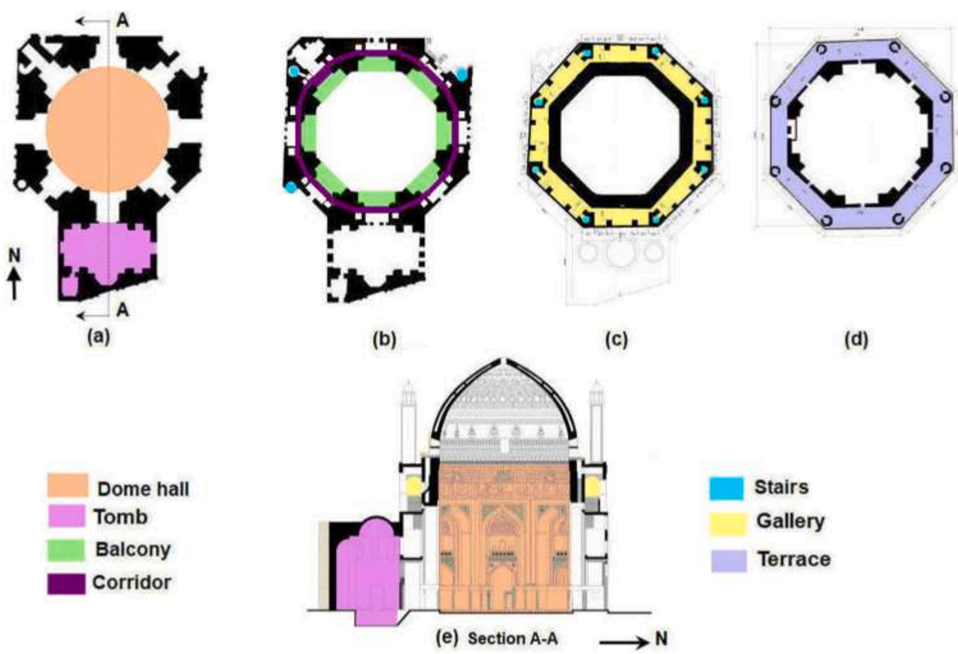

Fig. 3. Details of the different levels in the plan and cross-section: (a) Ground level; (b) First level; (c) Gallery level; (d) Terrace level; (e) Longitudinal cross-section.

colossal 47.5 m high dome is the earliest surviving example of its type. Its influence extended far beyond its location and became an important reference for the later development of domes all over the world. The dome of Soltaniyeh ranks among the largest domes constructed in the Middle Ages. It stands as the world's first highest double-shelled dome and the highest brick dome [60]. The use of double-shelled domes dates back to the Saljukid period (10th century). It is worth noting that before the construction of Soltaniyeh Dome, the outer shells were likely made of wood [61]. Beyond the Iranian world, the Pantheon in Rome (120–124 A.D.) boasts the highest and largest dome ever constructed in the ancient world, yet it lacks evident use of parallel shells [62]. The 30 m high Dome of the Rock (691–692 A.D.), in Jerusalem, displays a double-shell dome as well but it is built in timber rather than masonry [63]. The Dome of Santa Maria del Fiore in Florence is the most similar example to the Soltaniyeh Dome. Notably, Piero Sanpaolesi [4] suggested that the dome of Santa Maria del Fiore, with its use of a double-shelled structure, may have been inspired by that of Soltaniyeh. In fact, both structures, constructed in brick, were raised upon a central plan, featuring encircling chapels in the lower part of the building. The dome of Soltaniyeh, configured in a bulbous form, was built upon an octagonal plan. The octagonal plan is observed as well in Santa Maria del Fiore but its dome follows the same octagonal pattern as the base, incorporating eight ribs to support the structure. The construction system of Soltaniyeh, built almost a century before, could have reached Italy by the time Brunelleschi undertook the construction of the dome of Santa Maria del Fiore [4] (Fig. 2).

Soltaniyeh Dome is considered the best example of the architecture of the Ilkhanid era (1256–1335 A.D.). Its dome paved the way for further Iranian-style dome construction in the Persianate world, such as the mausoleum of Khaje Ahmad Yasavi in Kazakhstan, and the Taj Mahal in India.

2.1. Geometry and design

Geometric and structural properties of masonry buildings along with their construction techniques play an important role in their structural behavior [16]. From a design point of view, the plan of the Soltaniyeh mausoleum is a regular octagon. The mausoleum comprises four levels, see Fig. 3. The ground floor is covered by the dome, thus defining a large centralized space or dome hall (Fig. 3a). At ground level, the thickness of the main walls is 7 m. Two-story arcades encircle the domed main hall. Consequently, eight arches are visible on both the ground and first floors (Fig. 3e). The first floor includes eight balconies, one on each side, forming a kind of tribune that overlooks the interior. These balconies are

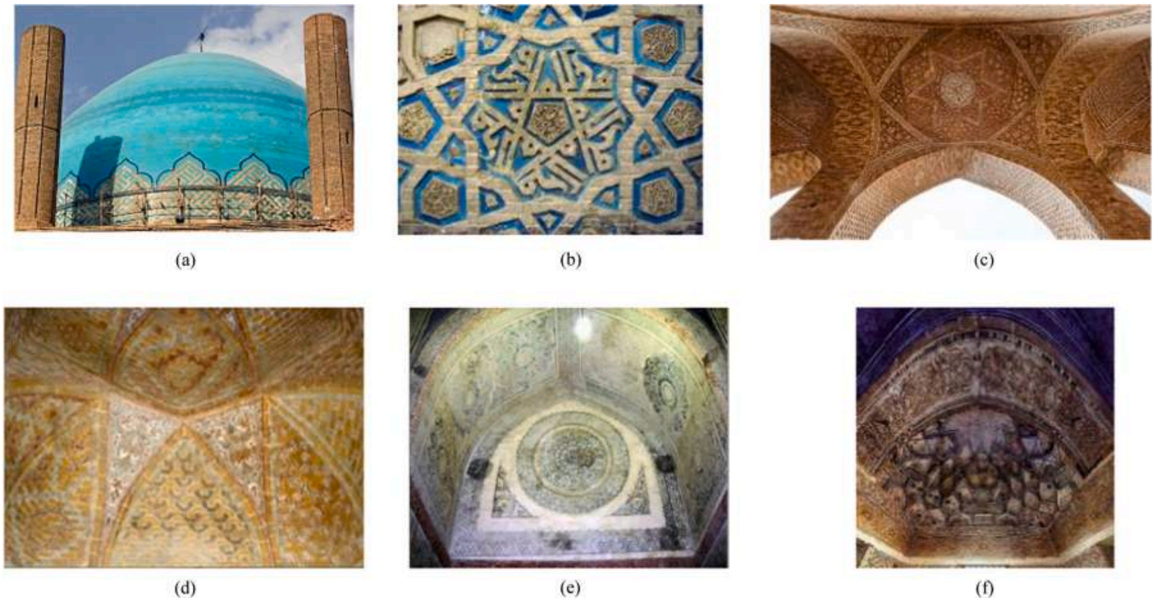

Fig. 4. Decorative works in the mausoleum: (a) Tileworks on dome; (b) Tile and brickwork decorations on walls; (c) Decorative vault's layers in the gallery; (d) Decorative brick work in the tomb; (e) Stucco decoration works in the tomb; (f) Suspended covering called Mogharnas [64].

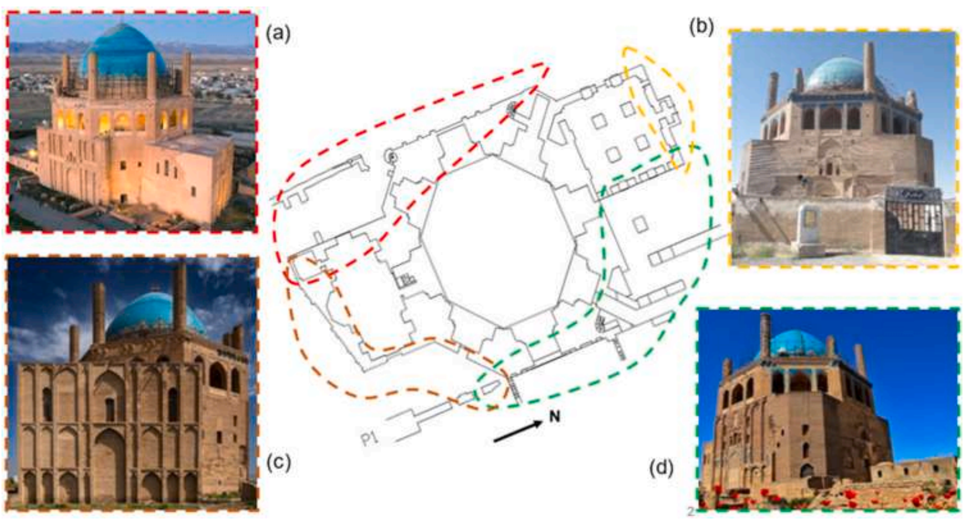

Fig. 5. External views of the mausoleum: (a) West facade; (b) North facade; (c) South facade; (d) East facade.

connected through a circular corridor, which can be accessed from the ground level by three staircases, two located on the western side and one on the eastern side (Fig. 3b). The north wall extends on either side of the ground and first floors, forming two triangular bodies that house staircases leading to the gallery encircling the building below a stalactite cornice (Fig. 3a and b). The second floor, or gallery level, features an octagonal gallery around the central space and below the great cornice (Fig. 3c). Each corner of this level encompasses a spiral staircase that continues up to the terrace level and the minarets above it. Each minaret has a diameter of 2.2 m (Fig. 3d and e). The terrace level (Fig. 3d) is the last floor and consists of an open space around the dome and drum. The dome has a span of 24.6 m and thickness of 1.7 m resulting in a 27 m outer diameter. It rises from the upper terrace to a height of approximately 47.5 m above ground level. The dome is standing on a massive platform without any buttresses or additional support.

The decorations of the mausoleum constitute another important facet of this monument, which is one of the most decorated buildings ever constructed in Iran. In particular, more than 10,000 m^2 of

Fig. 6. Similar configuration of the shrine built in Saudi Arabia by Iranian master builders [64].

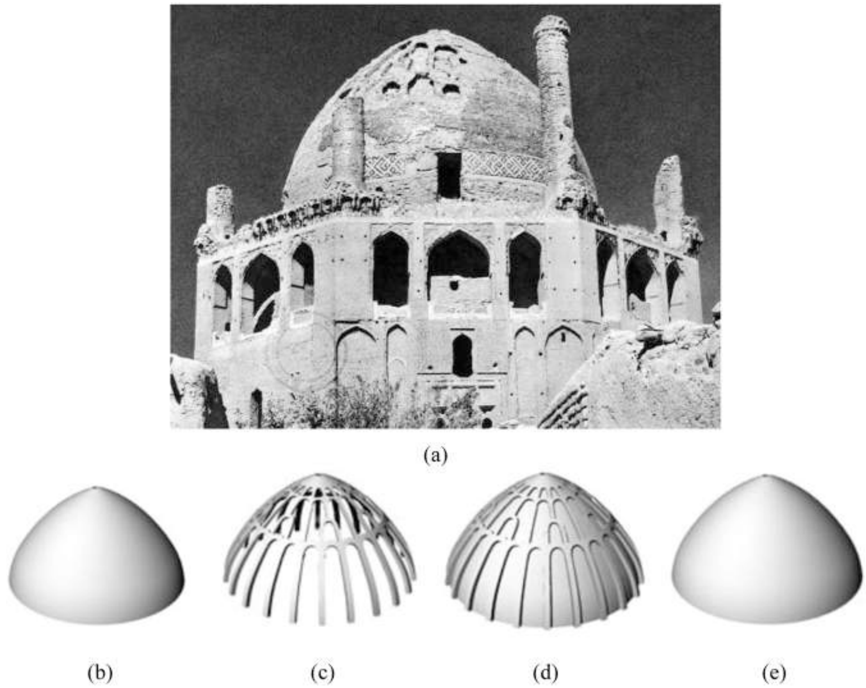

Fig. 7. Layers of the double-shell dome: (a) Box dome; (b) Inner shell; (c) Ribs network; (d) Inner shell + Ribs network; (e) Inner shell + Ribs network + Outer shell [66].

decoration cover the interior and exterior of the building. The existence of ornaments is likely to influence future strengthening decisions, if needed (Fig. 4).

The different facades of the mausoleum are presented in Fig. 5. In the northwest side of the mausoleum, a small mosque was built approximately a century, after the construction of the mausoleum (Fig. 5b). The presence of the eight minarets is a unique characteristic of Soltaniyeh mausoleum since this form has not been reported in any other building in Iranian architecture. Although some shrines built by Iranian master builders in Saudi Arabia share a similar form, albeit on a smaller scale, but these shrines were tragically ruined after 1925 due to religious beliefs (Fig. 6).

2.2. Construction techniques

The construction materials used in the building are brick, together with gypsum and lime-based mortar. As stated, the dome of Soltaniyeh is pioneer in choosing brick for the external shell as a building material since previous similar structures often utilized timber [65]. Notably, the construction of the double-shell dome of Soltaniyeh was among the first in Iran that employed a particular pattern of interlocking herringbone network. Thus, the type of double-shell dome of Soltaniyeh is a Box dome, which is a construction typology in which the connection of two separate shells is established through square lattice-shaped ribs, creating a unified and integrated structural element (Fig. 7). The Box system results in the reduction of the dome weight and associated gravitational load while it allows for covering a larger span. The presence of perpendicular connecting elements between the two shells, coupled with varying thicknesses of the outer and inner shells in specific locations, increases the stability and strength capacity of the dome [66]. In Box domes, the connected shells act as single-shell dome against compressive, torsional, lateral, and especially tensile forces. Given that minimizing tensile forces is a main concern in dome constructions, this particular structural arrangement proves optimal [66,91].

A unique characteristic of this dome is that the shells are parallel with a constant distance of 0.6 m and this parallel alignment of the shells is maintained even as their thickness decreases. As stated, the dome is surrounded by eight minarets on the terrace level. Minarets are the continuation of staircases that originate at the second level and are integrated with the surrounding wall up to the terrace level. The spiral stairs interlock with the staircase from the second level up to the terrace level and the minaret's cylinder.

The main structural system of the building is the so-called *Tagh va Tavizeh*, which is a combination of pointed arches, each spanning the gap between two adjacent columns, with squinches at the corners [91]. The squinches create a transition zone where the octagonal plan transforms into a circular shape where the dome starts. By using *Tagh va Tavizeh* structural system in addition to creating a proper base for squinches and the dome it would be possible to decrease the dimension of the surrounding structural walls and create void parts through the thickness of the walls. This also is beneficial for reducing the weight of the structure and decreasing the amount of required construction materials. Moreover, master builders mostly tried to combine this technique with aesthetic and artistic concepts. In the Soltaniyeh mausoleum, this technique has been applied using arches and openings and creating empty spaces, which are used as rooms and tribunes inside the thick walls.

The gallery is covered by two layers of vaults. The lower, visible vault is decorative and displays colorful bricks with different patterns, whereas the upper vault is the structural one. Considering the foundation of the building, very limited information is available. According to Kasaee [67], the foundation of the mausoleum is 2 m thick and consists of regular stone blocks and small irregular pieces of crushed stone with lime-based mortar.

2.3. Interventions

The Soltaniyeh Dome has undergone multiple conservation works during its life, primarily involving minor activities. According to the available records, the inner dome had been restored in the 1950 s. The most important and extensive intervention took place between 1969 and 1978, as a collaborative project between ISMEO, Italy, and Iran National University during which the main damages of the building, particularly the most relevant structural issues, were addressed. Traditional plaster

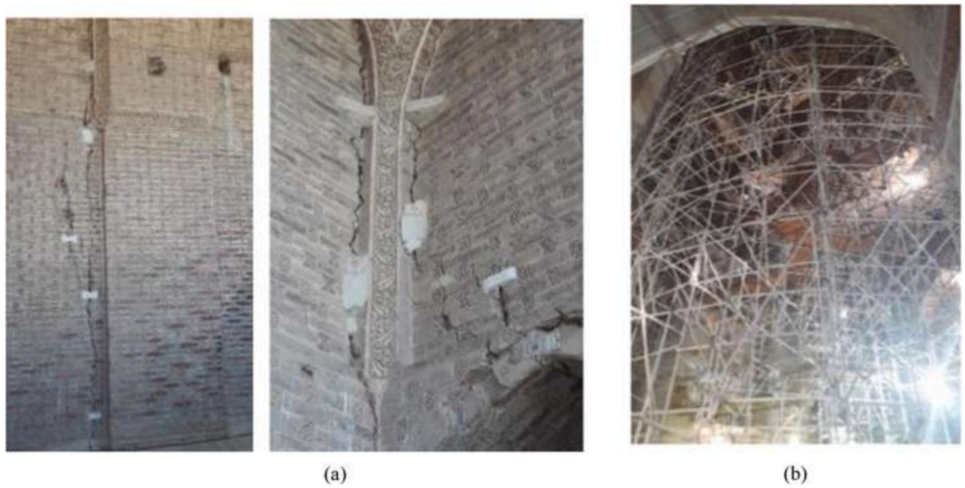

Fig. 8. Works during the 1960 s and 1970 s interventions: (a) Crack meters; (b) Scaffolding inside the dome hall.

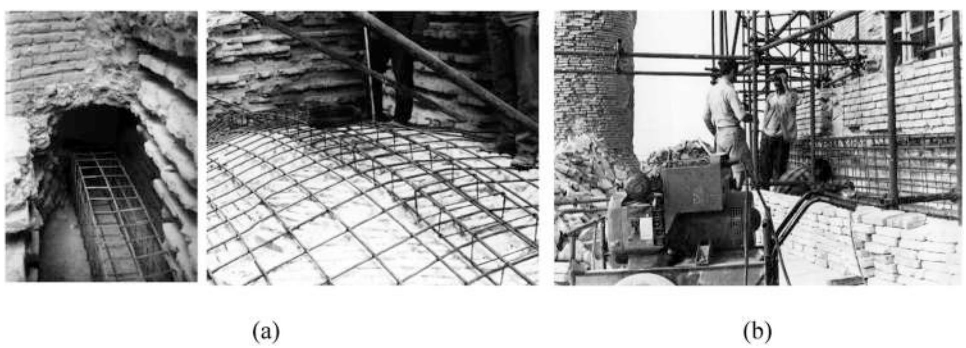

Fig. 9. Structural retrofitting during 1970 s intervention: (a) Reinforcement of vaults in the gallery; (b) Reinforced concrete ring [69].

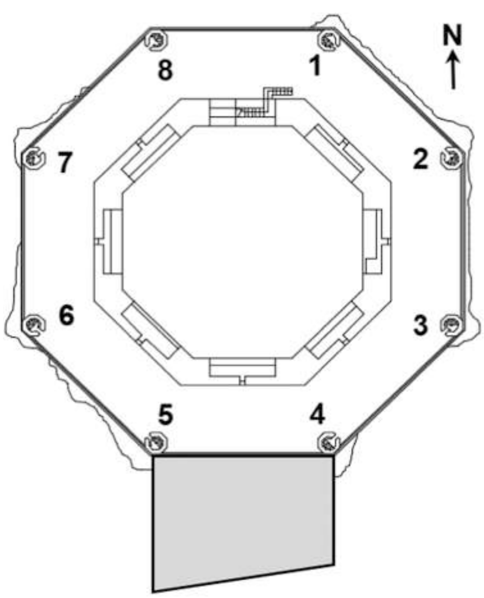

Fig. 10. Location and numbering of the minarets at the terrace level (tomb in grey).

crack meters were installed as monitoring devices to track changes and stability of cracks. Many of crack meters persist within the building (Fig. 8a). For these works, a massive scaffolding was installed inside the building and remains in place until the present day, which has facilitated the continued restoration of interior decorations (Fig. 8b).

The interventions within this past project can be divided into two categories. First, global activities aimed at improving the static behavior of the complex, such as repairing cracks and stabilizing elements that were prone to collapse. Second, a set of interventions aimed at retrofitting the entire structure was carried out. These included the strengthening of some vaults of the gallery by adding a layer of reinforced concrete (Fig. 9a), construction of a reinforced concrete ring (0.4 m thickness by 0.6 m height [68]) at the base of the dome (Fig. 9b), and the repair of cracks in the inner shell of the dome [69]. The second global restoration effort, primarily focused on the restoration of the artwork and the exterior facades of the mausoleum, was undertaken prior to its registration in the UNESCO World Heritage List in 2005.

Fig. 10 shows the location and numbering of the minarets around the dome at the terrace level. In the last decades, global conservation and structural retrofitting have been undertaken on the minarets.

As illustrated in Fig. 11, minarets 1, 3 and 7 are remains of the original ones, whereas minaret 2 is original, retrofitted with steel and a cement-based mortar. Around one-quarter of minaret 4 is original with the rest rebuilt, and minarets 5, 6 and 8 were completely rebuilt in past works.

3. Inspection works and diagnosis

Considering the available written and visual documents about the mausoleum, it is evident that the structure has suffered significant damages over time due to various factors. These damages have ranged from minor failures to the complete collapse of some parts. To investigate the present condition of the mausoleum, two visual site inspections

Fig. 11. Global conservation works and structural retrofitting of the eight minarets.

were carried out. The latest observations from these inspections indicate that crack meters have not recorded any significant movements. The existing cracks have not expanded, and no new major cracks have developed in the structure. The structural and decorative elements at risk of collapse have been fixed. The main structural damage of the building is the partial separation and collapse of the minarets, which has occurred over centuries (Fig. 11). Erosion and mortar loss are evident in the remains of the original minarets where covering tiles have also detached completely. Still, the overall structural condition of the building seems suitable. In the interior spaces, instances of material loss at the plinths of walls were observed, and general cracking was detected on the decorative materials covering the walls. The predominant damage in the

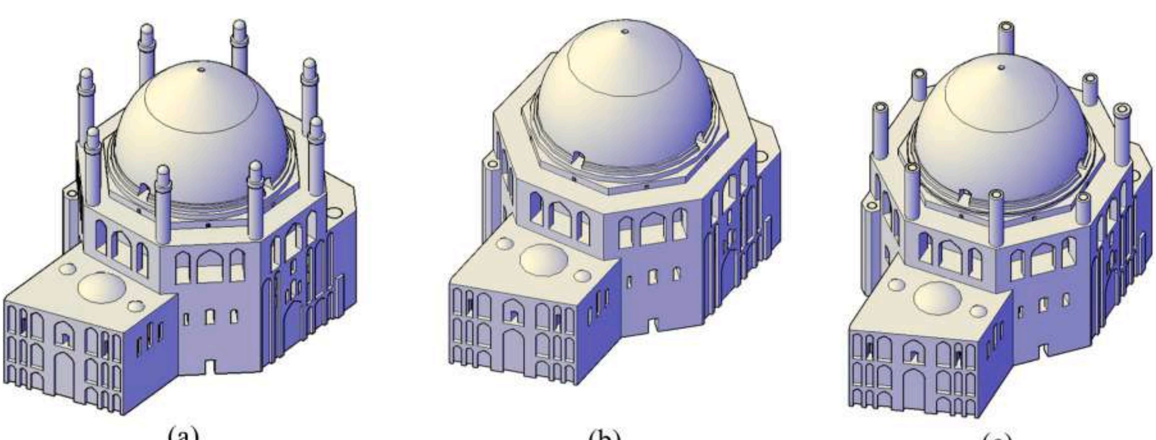

Fig. 12. Three-dimensional models of the mausoleum: (a) Original configuration (WM); (b) Original configuration without minarets (WOM); (c) Current configuration (CC).

Table 1
- Linear elastic and nonlinear properties of the materials used in the numerical models.

Material type	Density ρ (Ton/m^3)	Modulus of elasticity E (MPa)	Poisson's ratio ν (-)	Compressive strength f_c (MPa)	Compressive fracture energy G_c (N/mm)	Tensile strength f_t (MPa)	Mode-I fracture energy G_f (N/mm)
Material 1 (Masonry)	1.60	2000	0.15	3.60	5.76	0.17	0.016
Material 2 (Stairs)	0.48	600	0.15	1.08	2.61	0.05	0.012

tomb is the discoloration and development of crust on the plaster decoration. Collectively, the damage observed in the interior of the mausoleum can be classified as low, not threatening to cause any significant structural failures.

4. Preparation of the numerical models

Structural analysis is a strong tool to quantify and evaluate the behavior of structures under both static and dynamic loads. The analysis results are highly valuable in guiding the selection of appropriate repair methodologies and strengthening techniques. A numerical model consists of a model with a proper geometry in which material properties, applied loads, boundary conditions and finite element types as components of the numerical model have to be defined precisely, since they have a direct influence on the analysis process as well as analysis results. Numerical models are employed to investigate the global structural behavior of the structure and have to be able to account for the actual stiffness and mass distribution of the structure and to simulate the nonlinear behavior of the materials [48]. For the structural analysis of the Soltaniyeh Dome, several numerical models were prepared, and a series of analyses were performed to evaluate the structural response of the building.

4.1. Geometry

Following the objectives of the research, a comprehensive numerical representation of the structure was established through the preparation of three 3D models created in AutoCAD. The first model represents the original configuration of the mausoleum or pristine state before the partial collapse of the minarets and is called "model with minarets" (WM) (Fig. 12a). In the second model, the minarets have been removed completely. This modified model is referred to as "model without minarets" (WOM) (Fig. 12b). Finally, the third model represents the "current condition" (CC) of the structure considering the strengthening works and interventions (Fig. 12c). Due to the presence of decoration and non-structural elements, the models were prepared following a simplification strategy, with a primary focus on the structural elements. Since in box domes the two connected shells act as one integrated element the box dome considered as a massive single-shell dome. Additionally, the mosque adjacent to the building was assumed to have a small impact in the global response considering its scale, the presumably lack of connection with the main building (the mosque was built later) and the likely less stiff behavior (the walls of the main hall are 7 m thick whereas the walls of the mosque are below 1 m thick). Hence, none of the models include the mosque. For each of the cases, the corresponding geometry was imported into the Finite Element (FE) analysis software Diana FEA 10.6, where the numerical models were subsequently defined.

4.2. Material properties

In this study, two different materials have been defined. Material 1 encompasses the entirety of the mausoleum and the minarets. Due to the unavailability of direct characterization of the used construction materials, the properties of this material were defined according to the Iranian code [70] and data obtained from a similar structure where actual testing and dynamic identification were performed. The data also consider material degradation, since it was derived from testing the materials under real condition [16,30]. Material 2 is allocated to the staircases. As explained previously, the mausoleum includes 11 spiral stairs built with brick masonry like the one used for the rest of the structure. In order to reduce the complexity of the models, the spiral stairs have been substituted with equivalent cylindrical elements. Thus, the properties of Material 2 were calculated considering the volume fraction, v_f, that is by multiplying the corresponding values of the masonry by the relation between the volume of the original spiral stairs and the equivalent cylindrical elements, given by a ratio of 30 %. In other words, Material 2 was estimated based on the values of Material 1, multiplied this volumetric factor (Table 1).

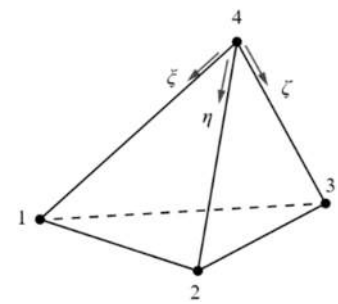

Fig. 13. TE12L, 4-node tetrahedron solid element used in the models.

4.3. Loads and boundary conditions

In the framework of this research, vertical gravitational load (self-weight) and the seismic load with horizontal pattern proportional to the mass of the structure defined by Eurocode 8 [71] were adopted. In order to define the boundary conditions, the translation of the base of the structure was assumed fixed in all directions.

4.4. Element type and mesh definition

The entire geometry was discretized using solid elements. In particular, the element TE12L, a four-node, three-sided isoparametric solid tetrahedron element, was selected as the primary meshing element type (Fig. 13). In order to optimize the number of elements of the model, mesh refinement was carried out both automatically and manually. This process considered crucial aspects for an accurate numerical model, such as the number of elements along the thickness of the structural elements and overall mesh optimization. Mesh sizes ranged from 0.15 m to 0.50 m, according to the dimensions of the structural elements.

4.5. Identification of damage

This research encountered various limitations. Due to the extensive scaffolding inside the dome hall, dynamic identification tests, which are a standard validation tool widely used to validate numerical models could not be performed. Instead, a linear static analysis under self-weight was performed on the structure to verify the initial

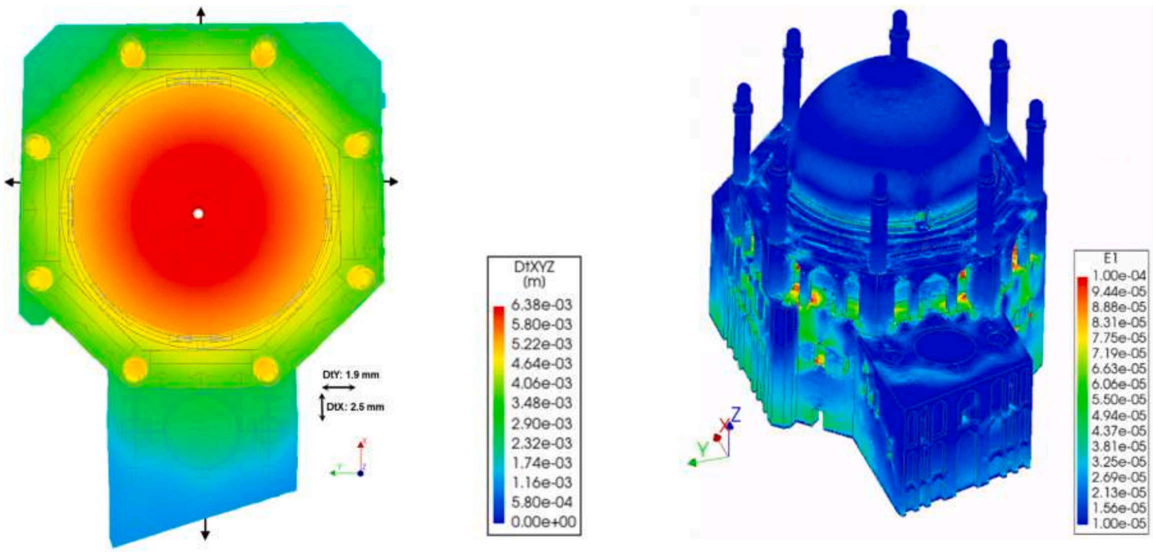

(a) Vertical displacements contour (also horizontal, Dtx and Dty).

(b) Maximum principal strains.

Fig. 14. Results of the linear static analysis for self-weight.

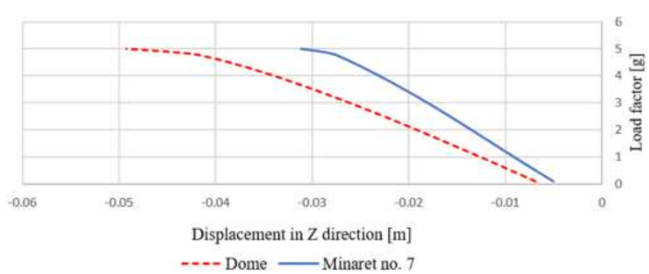

Fig. 15. Capacity curves for incremental vertical loading analysis in the WM model. Control points on top of the dome and on top of minaret number 7.

deformation and stresses at the base of the building. Hence, the self-weight was applied to the model and the displacement of the structure was obtained. For a point located in the middle of the east and south facades, the analysis results indicate that the maximum horizontal displacement in the X and the Y directions are equal to 2.5 mm and 1.9 mm, respectively (Fig. 14a). The uppermost part of the dome exhibits a maximum vertical displacement of 13 mm due to self-weight, while the top of the minaret experiences 7 mm vertical displacement. Maximum principal strains with the maximum values were found at the gallery level (Fig. 14b), but these values are rather low and indicate no cracking due to gravitational loading. Furthermore, visual observations did not reveal any significant cracks at the gallery level, although several restoration and repairs have been conducted on the structure including

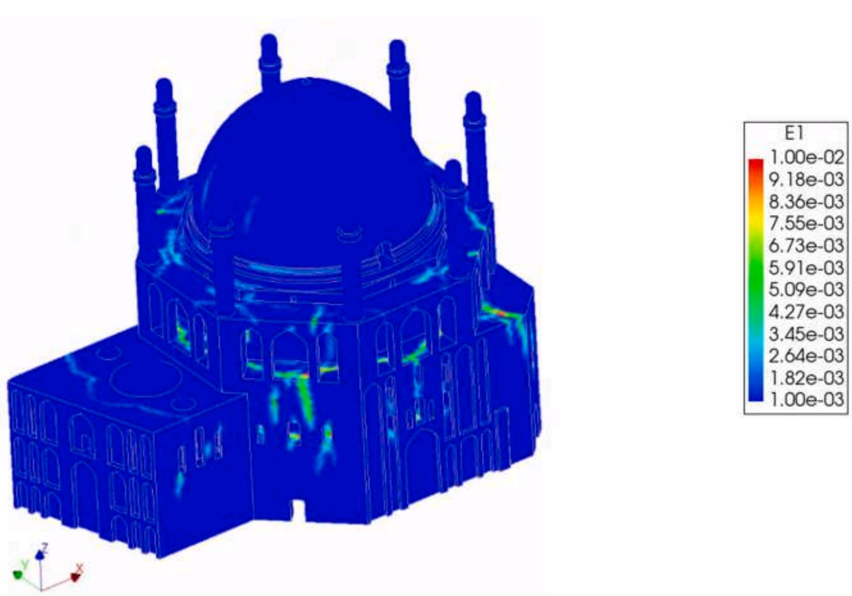

Fig. 16. Maximum principal strains at the end of the capacity curve (push-down analysis).

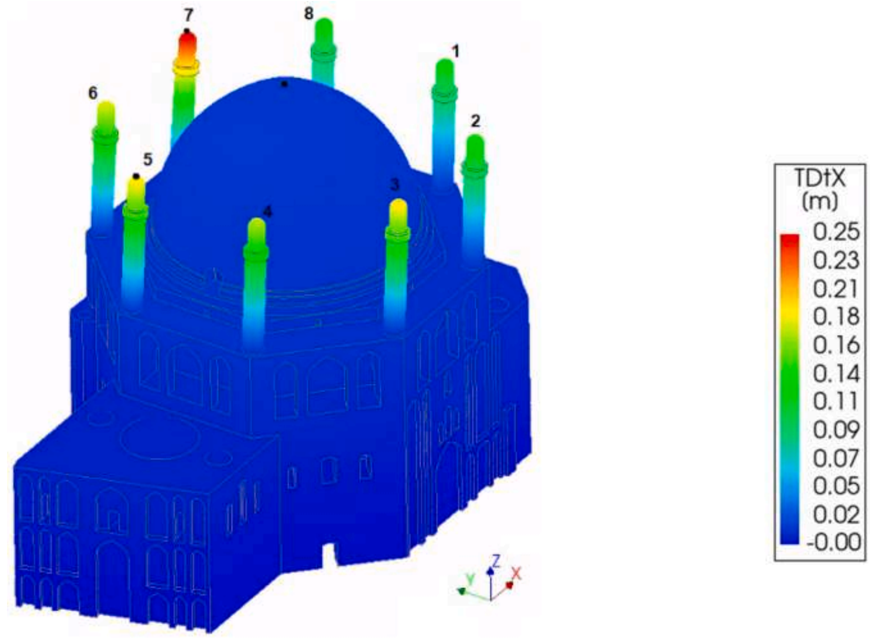

Fig. 17. Displacement in control points on top of the dome and minarets number 5 and 7.

the gallery level. It is likely that any probable damages had been repaired during past repair works. Considering maximum compressive stresses, the minimum principal stresses was identified at the base of the main walls, as expected. These are also small values, and much lower than the ultimate masonry strength.

4.6. Nonlinear analysis for incremental gravitational loading (push-down analysis)

In order to evaluate the stability of the structure, a nonlinear analysis for incremental gravitational loading was conducted. The first load step considered the total self-weight of the structure. Next, the gravity load was incrementally applied to the structure to assess the vertical loading capacity of the building. To control and evaluate the displacements throughout the analysis, reference points were established, namely a node on top of the dome and a node on top of minaret number 7. Fig. 15 illustrates the capacity curve of the structure, which can reach up to five times of its self-weight (5 g). The vertical displacement for the maximum load factor obtained for the control point on top of the dome is 50 mm, whereas the control point on top of minaret number 7 experiences a vertical displacement of 32 mm.

As illustrated in Fig. 16, damage is more pronounced at the gallery level over the vaults of the corridor, characterized by diagonal and horizontal cracks. In general, damage in the transversal direction of the structure is more prominent than the one in the longitudinal direction. Due to the possibility to increase gravity with a large factor, the global collapse of the structure due to the self-weight will not occur, even if some damage may develop at gallery level.

5. Seismic analysis

Soltaniyeh is located in a high seismic hazard zone [72], having experienced numerous strong earthquakes over the centuries. The building has undergone significant damage, notably the partial collapse of minarets which might have been caused by the past earthquakes in addition to the other causes of damage. The structural role and the seismic behavior of these minarets have always been under discussion.

The selection of an appropriate analysis approach is crucial when evaluating the load capacity and seismic behavior of existing structures. This choice significantly influences the necessary structural adjustments and the potential extent of damage in future seismic events.

Nonlinear time history analysis provides as a robust method for capturing the dynamic behavior of structures under seismic loads, offering a more realistic representation of structural response compared to pushover analysis by considering the time-varying nature of ground motion [73,74]. However, it is a complex and computationally intensive process, demanding substantial time and resources to execute, especially for complex, nonlinear and large-scale systems, making it impractical for regular use [73–78]. The accuracy of its results depends heavily on the selection of ground motion records and other input parameters, which may introduce uncertainty, complicating the utilization of results for retrofitting purposes [73]. For the Soltaniyeh dome, which contains a substantial internal scaffolding, determining number of signals, and the feasibility of conducting probabilistic seismic hazard assessment (PSHA) or macro zoning is highly intricate. Moreover, the complexity and vast scale of the Finite Element (FE) model significantly complicate and lengthen the time history analysis process. In the context of seismic analysis, pushover analysis emerges as a simplified alternative method that offers a less computationally demanding approach [79]. Therefore, the seismic performance of the entire structure including the minarets is investigated by means of nonlinear static, or pushover analysis, using the Finite Element (FE) software Diana FEA 10.6.

Pushover analysis, as a nonlinear static analysis, has been embraced by researchers as an effective alternative method [80]. It entails incrementally applying a pre-defined horizontal load pattern until a specified displacement target is achieved [80,81]. Unlike linear static analysis, pushover analysis considers nonlinear materials behavior and places specific focus on the verification of material models, making it particularly valuable for assessing masonry structures [82]. This analysis allows to determine the capacity of a structure to withstand horizontal loads [22]. Additionally, pushover analysis is considered a powerful tool, extensively used for assessment of structural behavior and seismic response of complex unreinforced masonry structures aiding in the identification of potential failure modes [16,22,29,83–85]. Recent developments in nonlinear algorithms, utilizing data from pushover analysis, demonstrate potential for generating more accurate seismic demand estimations with integration into contemporary seismic codes [71,86–89].

The whipping effect occurs when a lightweight structure is connected above a heavier one, provided that their frequencies are

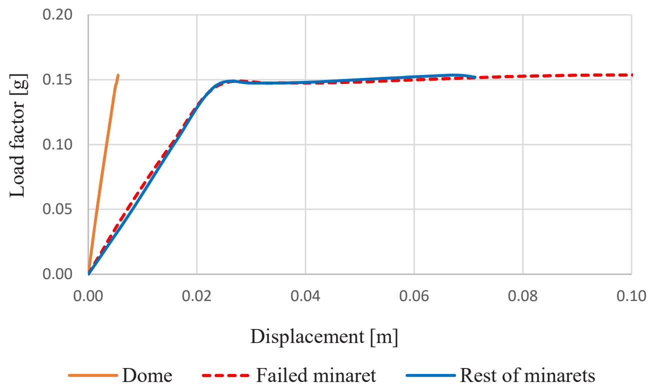

Fig. 18. Capacity curve for pushover analysis in +X direction in WM model. Control points on top of the dome, on top of the failed minaret (number 7), and on top of a sample minaret.

synchronized. This phenomenon can notably amplify seismic forces within the lighter structures. In the Soltaniyeh mausoleum the main period of the entire structure is 0.50 s and the main period of the minaret is 0.3 s. As per the Iranian code [70], the whipping effect is disregarded when the main period is below 0.70 s

The research process encompasses four main scenarios. The first scenario entails a nonlinear static analysis (pushover) conducted on the entire model of the mausoleum including the minarets (WM). This model seeks to simulate the behavior of the mausoleum in its original configuration. In the second scenario, all minarets along with the internal staircases were removed from the model (WOM), and pushover analyses were performed to discuss the performance of the main body of the mausoleum. The third scenario studies the structural behavior of the current configuration (CC) of the mausoleum by means of pushover analysis. This latter model accounts for the structural interventions made to the building. Finally, the seismic performance of the structure was further validated through limit analysis based on the kinematic approach.

In the models prepared for the Soltaniyeh Dome, the pushover analysis started with the application of the self-weight load in ten consecutive steps. Subsequently, the seismic loading was simulated through incremental application of horizontal forces until structural collapse. Various load steps were employed to achieve convergence of the equilibrium equation system. To accurately assess the response of

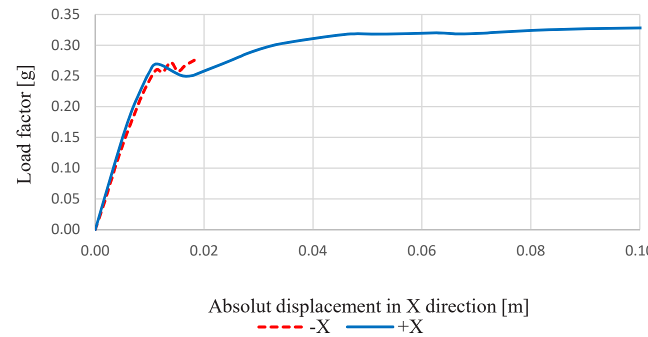

Fig. 20. Capacity curves for pushover analysis in +X and -X directions in the WOM model. Control point on top of the dome.

the structure, multiple control points were selected in all models. To attain equilibrium of the system of equations the Regular Newton-Raphson method was initially adopted, switching to the Secant iteration method in case of convergence difficulties.

5.1. Pushover analysis in the WM model in longitudinal direction (X)

The longitudinal direction of the building corresponds to the south-north axis, being south-north assumed the positive orientation, +X. Since the failure mechanism in both X and Y directions were found similar, only the result for the pushover analysis in the +X direction is presented here. For the purpose of explaining the failure mechanism obtained from the pushover analysis in +X direction, results are presented for three different points, namely on top of the dome (as a reference control point for all other analyses), on top of the weakest minaret, and on top of one of the other minarets at maximum load factor (Fig. 17). The capacity curves presented in Fig. 18 shows that the structure reaches a maximum load factor of 0.15 g. At this load level, the dome has a minor displacement of 5 mm, whereas the displacement in minaret number 7 reaches more than 0.20 m, and the remaining minarets experience displacements around 0.07 m. Consequently, in the +X direction, the critical failure mechanism is observed in minaret number 7, even if the rest of the minarets also fail.

The maximum principal strains were used to evaluate crack patterns and collapse mechanisms. As illustrated in Fig. 19, damage is more pronounced at the base of the minarets, characterized by diagonal and horizontal cracks, while minor damage appears on the main arches in

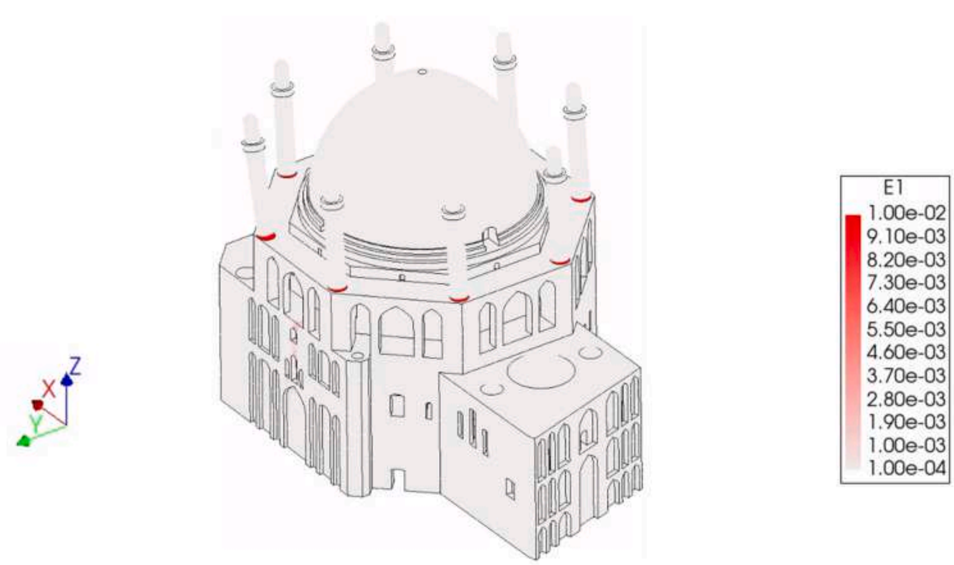

Fig. 19. Maximum principal strains for the WM model in the +X direction at the end of the capacity curve. Def. factor: 20.

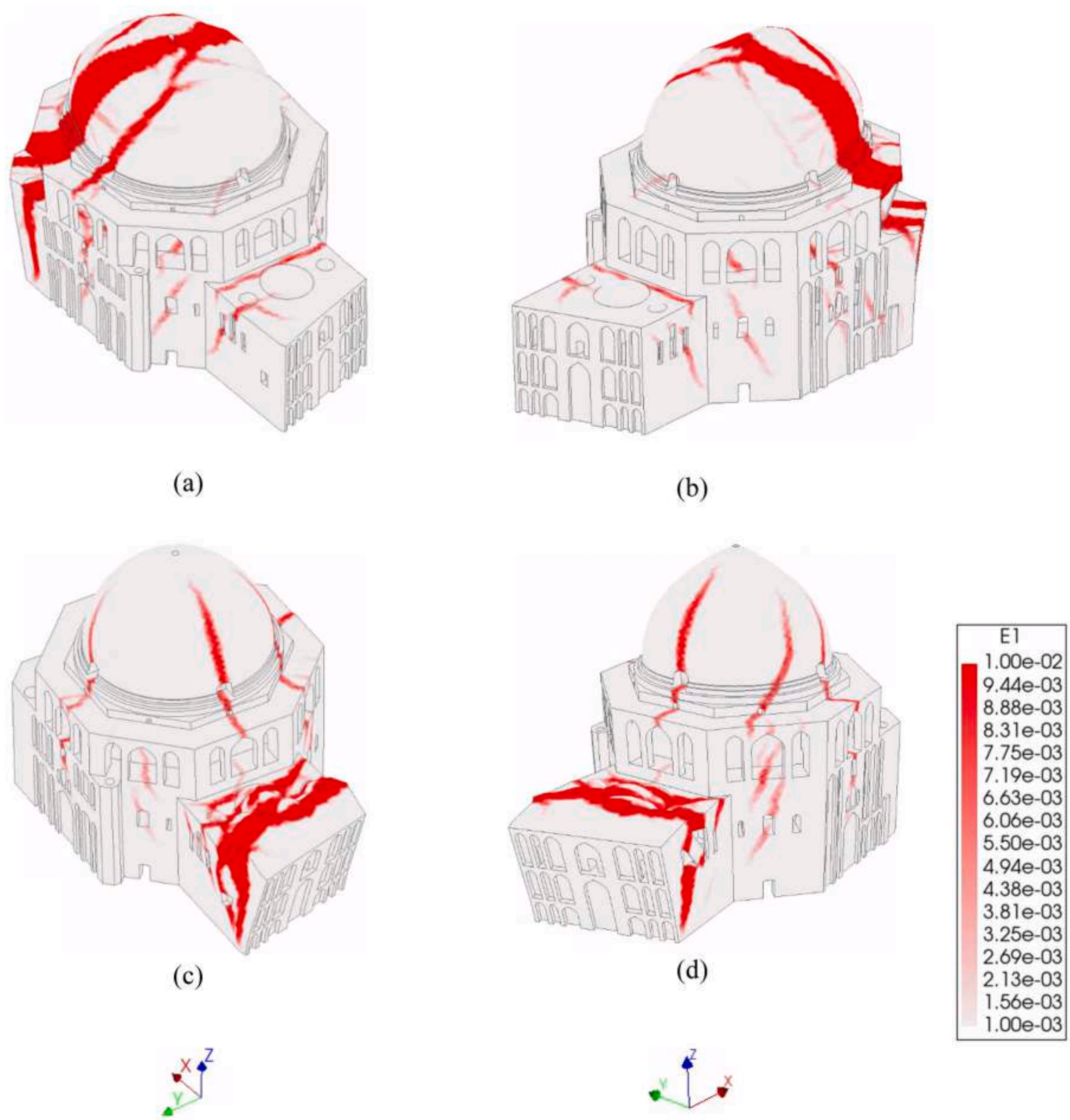

Fig. 21. Maximum principal strains for the WOM model in the +X (a, b) and -X (c, d) directions at the end of the capacity curves. Def. factor: 50.

the first and second floors. It is noteworthy that the local collapse of minaret number 7 is marked by distributed horizontal cracks at its base. The masonry walls of the dome hall do not present any damage at this level of lateral load. Furthermore, no damage is identified on the dome nor in the tomb. In general, the analysis results reveal that the main damage is concentrated at the base of the minarets. The extent of damage at the base of the minaret number 7 is notably more severe since the structure in this part presents some asymmetry and the wall supporting this minaret is thinner compared to the other walls of the octagonal structure.

5.2. Pushover analysis in the WOM model in the longitudinal direction (X)

The capacity curve illustrated in Fig. 20 shows that the structure presents a maximum load factor of 0.33 g in the positive direction and maximum load factor of 0.27 g in the negative direction, representing 18% reduction. In the -X direction, failure occurs in the tomb, with the maximum displacement observed in that area. Consequently, the control point on top of the dome registered a minor displacement of 17 mm at maximum load factor, whereas a point on the uppermost part of the tomb, where failure occurred, exceeded the limit displacement of 0.10 m for the same load factor.

In terms of the damage patterns in the positive direction (Fig. 21a, b), damage is more widespread and is characterized by diagonal cracks. This damage encompasses the dome, together with the north-east and the north-west corners of the structure. Therefore, local collapse of the dome and the two main arches in the corners of the north wall is observed. Conversely, the analysis results for the -X direction (Fig. 21c, d) presented vertical cracks in the dome, diagonal and horizontal cracks in the tomb, and damage at the connection between the dome hall and the tomb. Moreover, the masonry walls of the south facade do not present any damage. In general, the damage obtained from the pushover analyses in the +X direction is primarily concentrated within the dome and the north corners, and in the tomb in the -X direction. Cracks predominantly show a characteristic shear diagonal pattern, but vertical cracks are evident on the dome as well, extending downward through the transition zone and continuing through the main arches. Damage is

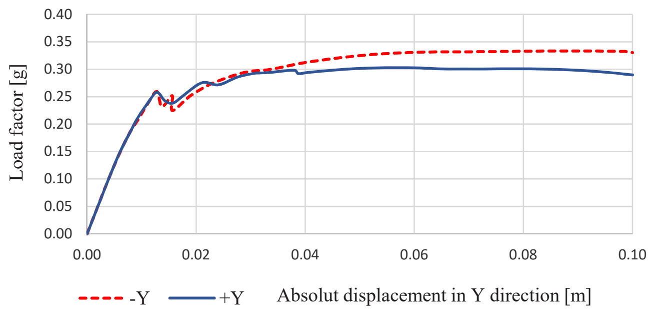

Fig. 22. Capacity curve for pushover analysis in +Y and -Y directions for a point on top of the dome in the WOM model.

also observed at the base of the surrounding north and south walls, for both positive and negative directions.

5.3. Pushover analysis in the WOM model in transversal direction (Y)

The transversal direction of the building corresponds to the east-west axis, being east-west assumed as the positive orientation, +Y, and the opposite, -Y. The capacity curve depicted in Fig. 22 shows that the structure presents a maximum load factor of 0.29 g in the positive direction and a slightly higher maximum value, up to 0.33 g, in the opposite direction. The damage pattern resulting from these analyses is presented in Fig. 23. In +Y direction, diagonal meridian cracks are observed on the dome, extending downward through the drum and the transition zone, ultimately passing through the main arches of the second and first floors. These diagonal cracks develop in a cluster shape and become more severe in the corners of the dome hall. Additionally, hoop cracks are visible in different heights of the dome. Horizontal cracks are identified in the connection zone of the drum and the roof floor, as well as at the base of the main west walls. In the tomb area, diagonal and horizontal cracks appear through the small domes and west vault. Finally, diagonal cracks spreading from the corners of the openings are also visible in the tomb (Fig. 23a, b).

The results of the analysis in -Y direction reveal similar damage patterns (Fig. 23c, d). Diagonal cracks on the dome spread downward through the drum and the transition zone, ultimately passing through the main arches of the second and first floors. Nonetheless, these cracks are less severe in the corners when compared to the +Y direction. Hoop cracks are visible near the base of the dome. Horizontal cracks are present in the connection zone between the drum and the roof floor as well as in the base of the main east walls. Diagonal cracks are observed in the eastern part of the tomb, together with a concentration of diagonal cluster cracks around the corners of the openings. In general, the evaluation of the analysis in the -Y direction reveals comparatively lesser damage than that observed in the +Y direction.

5.4. Pushover analysis in the CC model in longitudinal direction (X)

The objective of this analysis is to assess the seismic behavior of the mausoleum in its current configuration to the fullest extent possible,

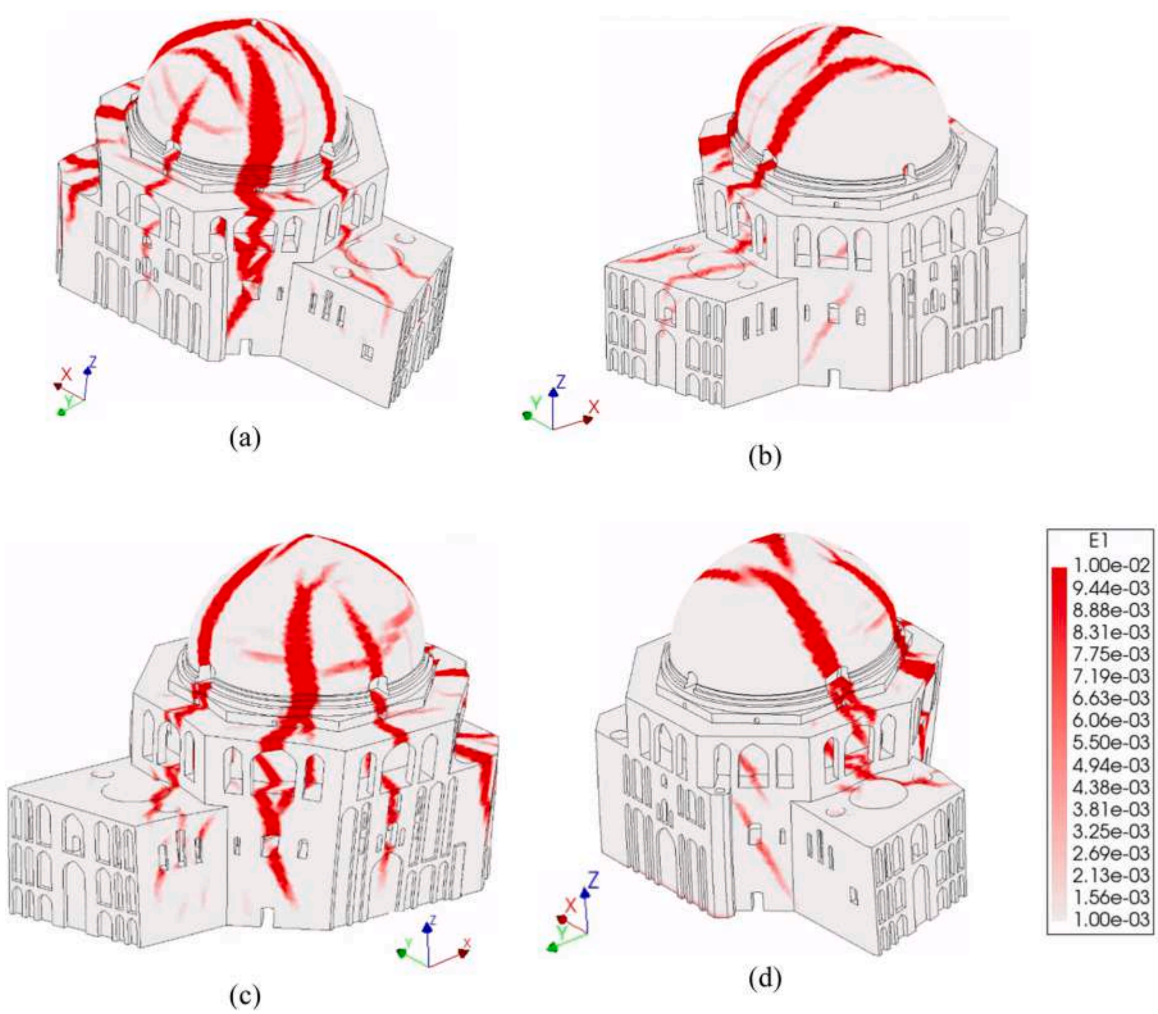

Fig. 23. Maximum principal strains for the WOM model in the +Y (a, b); and -Y (c, d) directions at the end of the capacity curves. Def. factor: 50.

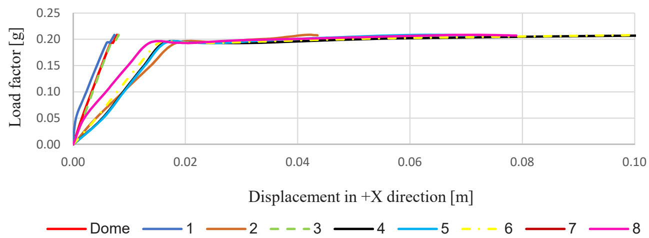

Fig. 24. Capacity curve for pushover analysis in the +X direction in the current configuration model. Control points on top of the dome and minarets.

despite limited information. Since the failure mechanism in both longitudinal and transversal directions were similar, hence results just for the pushover analysis in the positive longitudinal direction are presented. Regarding the interventions that have been performed in the mausoleum, a reinforced concrete ring was built below the base of the dome. In addition, minaret number 2 has been strengthened using steel belts, vertical steel elements and cement-based mortar. Minarets number 4, 5, 6 and 8 have been totally or partially reconstructed with masonry, while numbers 1, 3, and 7 are remains of the original ones. Unfortunately, detailed data concerning design specifications, concrete and steel properties, and other related information were not accessible for inclusion in the model. To account for the effects of the aforementioned interventions and structural changes within the model, the concrete ring and minaret number 2 were represented as elements with fully elastic behavior. The rest of the elements were assigned the reference nonlinear material properties. Fig. 24 presents the capacity curve of the structure for a point on top of the dome and top of each minaret. The structure attains a maximum load capacity of 0.21 g, with a corresponding maximum displacement of 8 mm for the top of the dome. Minarets number 1 and 3, both original, experience the same displacement as the dome, while minaret number 7, also original, undergoes a displacement of 45 mm. This confirms the results from the previous analyses on the model with minarets, indicating that minaret number 7 is susceptible to collapse against lateral loads. The strengthened minaret

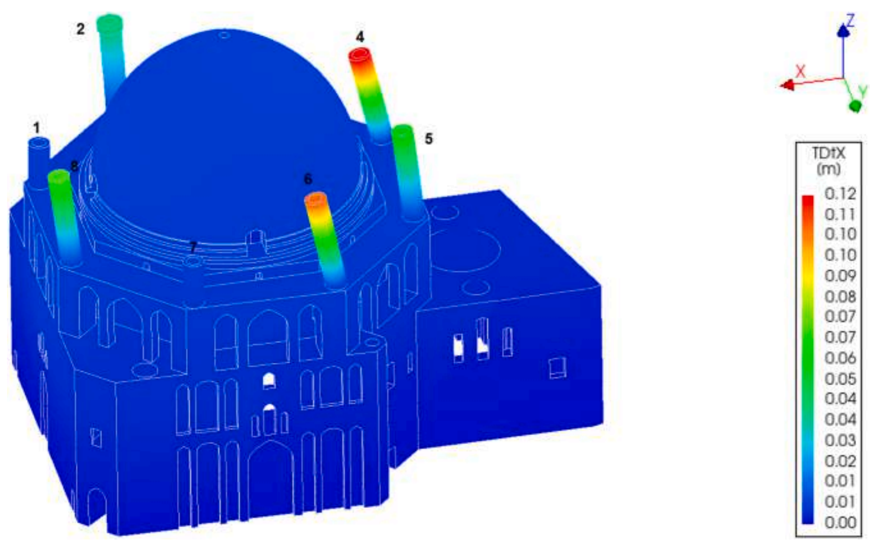

Fig. 25. Displacement of the minarets at maximum load factor. Def. factor: 20.

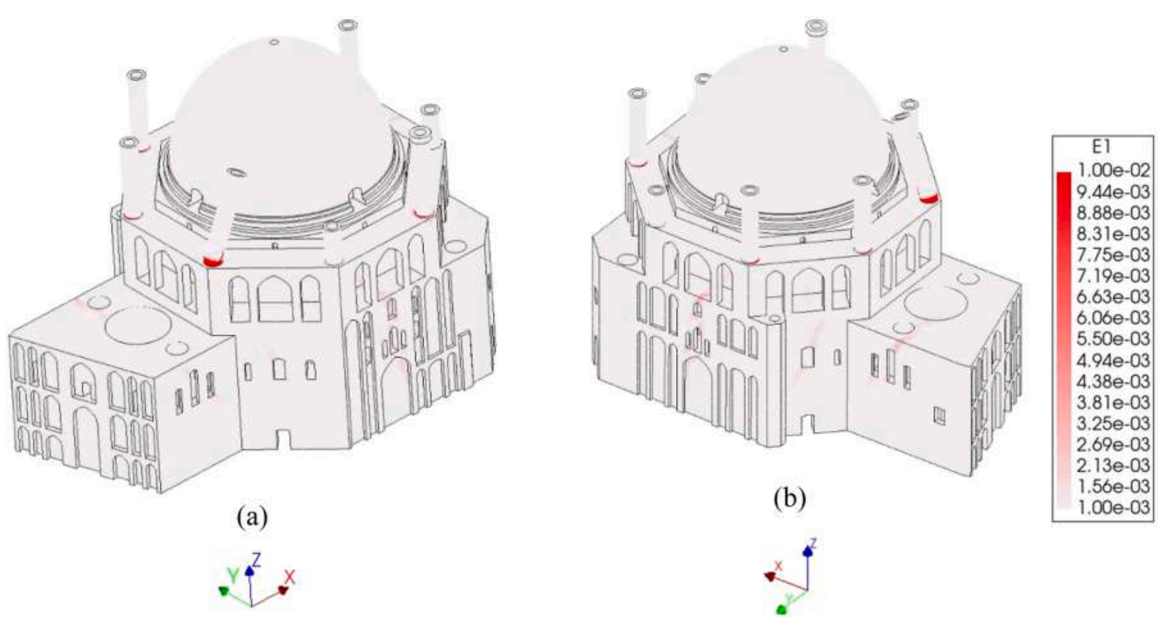

Fig. 26. Maximum principal strains for the current configuration model in the +X direction. (a) East view; (b) West view. Def. factor: 20.

number 2 experiences a displacement of 44 mm at maximum load factor. This high value for displacement can be attributed to the lack of connection between the steel ties and the base, since the consolidation focused solely on the upper part, neglecting the connection between the base of the minaret and the roof. Consequently, the stiffness and mass of the retrofitted portion are higher than the lower part, possibly leading to the concentration of damage at base and subsequent collapse. Minarets number 4, 5, 6 and 8, which were reconstructed, experience displacements of more than 80 mm at maximum load factor. In general, minarets present higher displacements compared to the main body of the mausoleum, where displacement remains minimal (Fig. 25).

Fig. 26 presents the obtained damage pattern in this analysis. Diagonal and horizontal cracks are evident at the base of all minarets, more pronounced at the base of the taller minarets. Diagonal cracks are visible through all the main arches from top to bottom. Furthermore, concentration of diagonal cracks also affects the corners around the openings. In comparison to the previous analyses on the models WM and WOM, the results from this analysis reveals less damage, notably the absence of horizontal and vertical cracks at the base of the dome and roof level. Moreover, no cracks appeared in the interior of the mausoleum. This can be attributed to energy dissipation facilitated by the elastic structural elements, namely the reinforced concrete ring, enhancing the global elastic behavior and ductility of the overall system.

5.5. Limit analysis

The limit analysis with macro-blocks is a simplified and powerful structural analysis tool to evaluate the ultimate capacity of masonry structures by static models, involving the equilibrium of the macro-blocks through the limit analysis basic concepts. A macro-block corresponds to a portion of structure with similar material properties and structural behavior, which can represent the structural element or a set of structural elements [48]. After conducting pushover analyses, the seismic behavior of the structure was further investigated through limit analysis based on the kinematic approach. Limit analysis should allow to calculate an estimate of the collapse load. Furthermore, the limit analysis requires a reduced number of input parameters, which is an advantage for the assessment of ancient and historical masonry structures, due to the difficulties in obtaining reliable data [48].

To define the collapse mechanisms, the proposed methodology outlined in NIKER D3.1 [90] was applied considering the results from the numerical analyses and existing damages and irregularities in the building. The structure was discretized and four different collapse mechanisms were identified, also considering the pushover analyses. Mechanisms 1 and 2, which correspond to the belfry and the minaret, were considered for the model with minarets (Fig. 28a and b in Gray). Conversely, mechanisms 3 and 4 were proposed for the model without minarets (Fig. 28d and e in Gray). Description of the mechanisms is given as following:

- Mechanism 1: Overturning of the belfry with rotation at the base (Fig. 28a).
- Mechanism 2: Overturning of the minaret with rotation at the base (Fig. 28b).
- Mechanism 3: Overturning of the tomb with rotation at the base of the south facade (Fig. 28c and d).
- Mechanism 4: Overturning of the dome and north facade with rotation at the base of north facade (Fig. 28c and e).

To calculate the load multipliers for the selected mechanisms, a 3D model of the elements or components involved in each mechanism was created. This was accomplished either directly (Mechanisms 1 and 2) or by cutting the reference 3D model (Mechanisms 3 and 4) in AutoCAD software. Subsequently, the weights of these elements were calculated based on their volume and mass, and the center of mass for each element was determined. The load factor a_0 that activates the mechanism was obtained through the division of the resistant moment (MR) by the overturning moment (MO).

The location of the hinges and the mass contribution of the elements needs to be computed before calculating MR and MO. The computations of the values were performed using Eqs. (1) to (4) where γ_m is the material partial safety factor, FC is the confidence factor related to the level of knowledge of the structure here considered as the unit value, e^* corresponds to the mass participation factor of the mechanism, d_1 and d_2 represent the position of the hinge within the thickness of the corresponding wall, assuming the compressive strength of the material and a triangular and a rectangular distribution of stresses, respectively, whichever is larger, M^* is the mass that participates in the mechanism, P_i is the vertical component of the self-weight and $\delta_{x,i}$ is the virtual horizontal displacement of the center of mass of the macroblock i.

$$\sigma_c = \frac{f_c}{FC\cdot\gamma_m} \tag{1}$$

$$d_1 = \frac{2\cdot\sum_i W_i}{3\cdot\sigma_c\cdot L}, d_2 = \frac{\sum_i W_i}{2\cdot 0.8\cdot\sigma_c\cdot L} \tag{2}$$

$$e^* = \frac{g\cdot M^*}{\sum_i Pi} \tag{3}$$

$$M^* = \frac{\left(\Sigma_i P_i \delta_{x,i}\right)^2}{g\Sigma_i P_i \delta x_{i,1}^2} \tag{4}$$

Once the collapse mechanisms and corresponding load multipliers were defined, a force-based assessment was performed to verify the stability for each of the considered mechanisms using the procedure defined in the Italian code NTC-18 [52]. The code-based assessments were performed for Ultimate Limit State (ULS) according to the following two verifications:

I. Mechanisms involving part of the structure in contact with the soil:

$$a_0^* \geq \frac{a_{gR}\cdot\gamma_I.S}{q} \tag{5}$$

II. Mechanisms involving part of the structure above ground level:

$$a_0^* \geq \frac{S_e(T_1).\psi(z).\gamma}{q} \tag{6}$$

Therefore, verification II was considered for Mechanisms 1 and 2, whereas verification I was applied for the Mechanisms 3 and 4. In Eq. [5] above, a_0^* stands for the spectral acceleration required to activate the mechanism, a_{gR} identifies the peak ground acceleration (PGA) based on seismic zonation, modified by γ_I, known as importance coefficient, set equal to 1.2 according to the Iranian Code 2800 [72], S is the soil coefficient, and q stands for the behavior coefficient, assumed as 2 according to the code. Additionally, in the following equation $S_e(T_1)$ defines the spectral acceleration associated with the first mode of vibration of the structure (obtained from eigenvalue analysis) in the corresponding direction, $\psi(z)$ is the ratio of the center of the mass to the total height, and γ is an amplification factor that considers the number of floors. The spectral acceleration that activates the mechanism is determined as follows:

$$a_0^* = \frac{a_0\cdot g}{e^*\cdot FC} \tag{7}$$

where g corresponds to the acceleration of gravity (9.81 m/s^2), and a_0 is the load factor that activates the mechanism (determined by the Principle of Virtual Works for the equilibrium between the MO and MR).

The verification of the structural safety for the seismic action was carried out using the values obtained from the Iranian Code 2800 [72] (Table 2). The building spectrum coefficient S_e, which characterizes the

Table 2
- Predefined values from the Iranian Code 2800 [72].

Ground Type	$T_B(s)$	$T_C(s)$	S_0	S	η
B	0.15	0.50	1.00	1.50	1.00

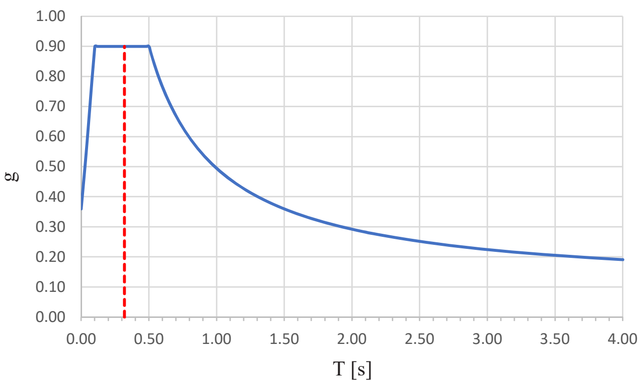

Fig. 27. Elastic response spectrum for ground type B according to the Iranian code and the natural period of the building.

Table 3
- Results of safety verifications I and II (V: Verified, NV: Not verified).

Mechanism	Maximum load factor a_0 (g)	Maximum capacity a_0^* (m/s^2)	Demand capacity a_{fb} (m/s^2)	Verification
Mechanism 1	0.54	5.35	5.56	NV
Mechanism 2	0.17	1.66	4.65	NV
Mechanism 3	0.24	2.35	2.70	NV
Mechanism 4	0.23	2.30	2.70	NV

Table 4
- Safety verification for seismic action based on the results obtained from pushover analysis (V: Verified, NV: Not verified).

Model type	Loading direction	Maximum load factor a_0 (g)	Maximum capacity a_0^* (m/s^2)	Demand capacity PGA (m/s^2)	Verification
Original model with minarets	+X	0.15	1.47	3.00	NV
Model without minarets	+X	0.33	3.23	3.00	V
	-X	0.27	2.64	3.00	NV

response of the building to ground motion, is a function of natural period T and the ground type. The natural period of the building is equal to 0.32 s (obtained from eigenvalue analysis) and the ground type of the region is the type B.[1] In Table 2, T_B and T_C are limit values for period obtained from the code and depend on the soil type and the natural period of the structure, S_0 and S are the minimum and the maximum of the soil factor, and η is the mode shape modification coefficient dependent on the distance of the fault from the building, typically considered 1 for 5% damping. The seismic hazard assessment for the site, based on probabilistic hazard evaluation, primarily considers earthquakes with a surface-wave magnitude, Ms, greater than 5.5. Hence, the structural safety verification for the seismic action was focused exclusively on the Type I spectrum (Fig. 27). Eq. (8) describe the spectrum.

$$
\begin{aligned}
S_e(T) &= a_{gR}\cdot\gamma_I\cdot\eta\cdot\left(S_0 + (S - S_0 + 1)\left(\frac{T}{T_B}\right)\right) && 0 < T < T_C \\
S_e(T) &= a_{gR}\cdot\gamma_I\cdot\eta\cdot(S+1) && T_B < T < T_C \\
S_e(T) &= a_g\cdot\gamma_I\cdot\eta\cdot(S+1)\left(\frac{T_C}{T}\right) && T > T_C
\end{aligned}
\tag{8}
$$

The stability of the structure is analyzed considering the load factor that activates the collapse mechanism in terms of maximum horizontal acceleration and the demand acceleration. According to the force-base procedure, the acceleration capacity, a_0^*, has to be greater than or equal to the demand acceleration, a_{fb}, in order not to violate the safety criteria. Table 3 presents the results of verification II for Mechanisms 1 and 2 and verification I for Mechanisms 3 and 4.

5.6. *Comparison of limit analysis results with nonlinear static analysis results*

As presented in the results of pushover analyses, the structural failure in the original model (WM) is associated with the collapse of the minarets, primarily initiated by the failure of minaret number 7 (Mechanism 2). Regarding the WOM model, the collapse mechanism in the -X direction involves the southern structures of the tomb (Mechanism 3). Conversely, the collapse mechanism in +X direction involves the northern section of the mausoleum, including the dome and the north wall corners (Mechanism 4).

In order to evaluate the stability of the structure the maximum capacity in terms of horizontal acceleration on the structure and the demands in terms of Peak Ground Acceleration (PGA) are compared. Table 4 presents the results of the pushover analyses for the WM and WOM models. According to the Iranian code [72] the demand capacity for the region is 3 m/s^2. For the WM model, the lowest horizontal acceleration of the structure, 0.15 g, is observed for the seismic action in the +X direction. As is presented in Table 4 since the maximum capacity of the building is less than the demand capacity thus, the minarets do not meet the required safety verification for the considered earthquake. This is further confirmed by the results of the force-based control limit analysis. Considering the results of the pushover analysis in +Y and -Y directions (Fig. 23), the failure mechanisms involve complex combinations of several meridian cracks initiating on the dome and propagating downwards through the structure. This complexity poses challenges for defining and evaluating the mechanism accurately. Consequently, the assessment in the transversal direction was not performed in this research.

It is noted that in the pushover analyses the minaret behaved as a unique element. Conversely, two mechanisms were considered for the limit analysis, including an additional mechanism for the upper section or belfry. This additional mechanism is not directly comparable to the pushover analysis results. When comparing the maximum load capacity between limit analysis and pushover analysis, the latter presents higher values. These discrepancies could be attributed to energy dissipation caused by complex cracks propagating in various directions. Moreover, the volume considered for the macroblocks based on pushover analysis may not completely replicate the actual macroblocks. Based on the available information in Table 3 and Table 4, it can be inferred that the safety of the minaret in both cases is not confirmed. In the case of the

[1] . Very compact soil or loose rock, including sand, very dense sand, very hard and thick clay with more than 30 m of thickness, exhibiting gradually improving mechanical specifications with increasing depth.

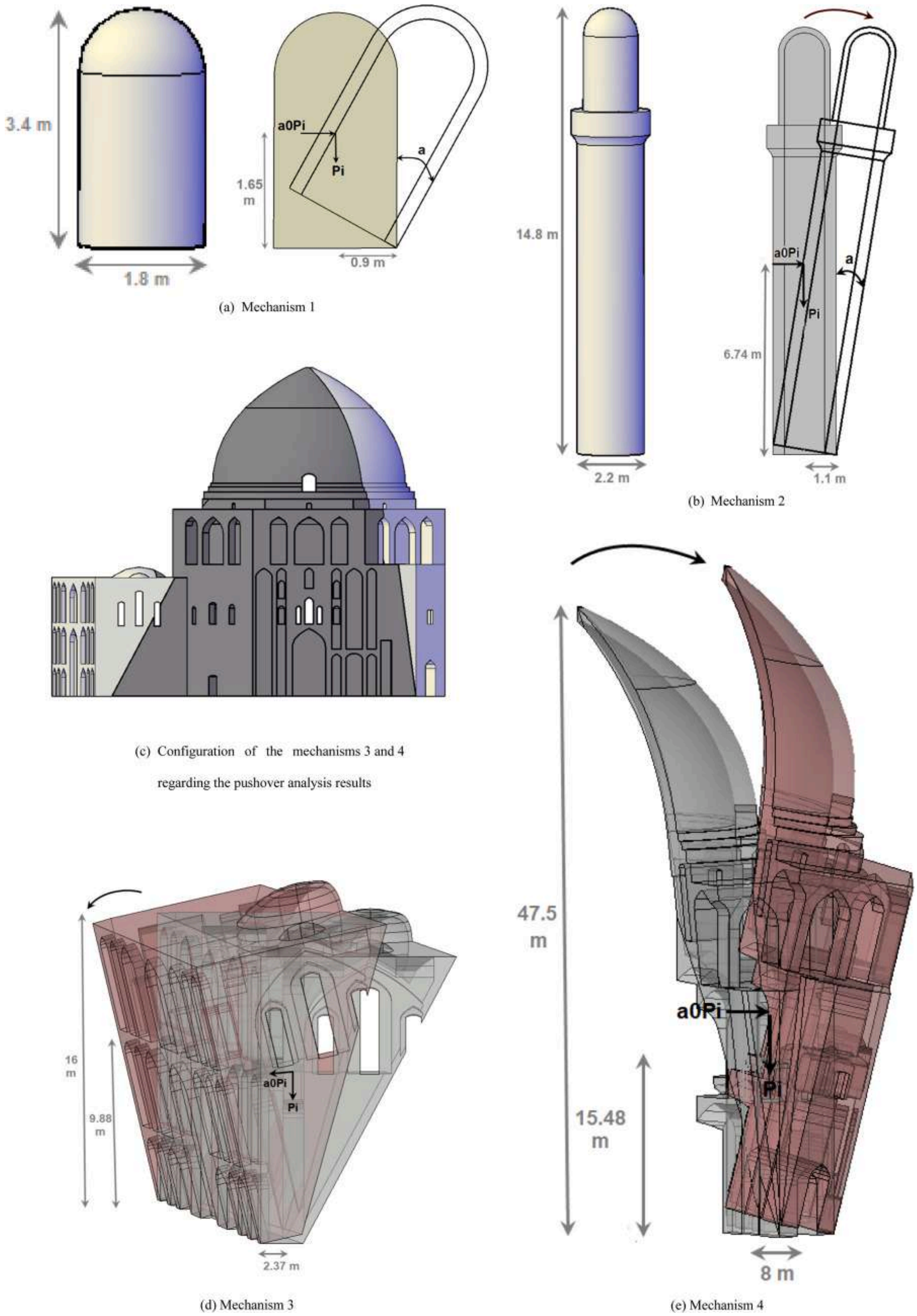

(a) Mechanism 1

(b) Mechanism 2

(c) Configuration of the mechanisms 3 and 4 regarding the pushover analysis results

(d) Mechanism 3

(e) Mechanism 4

Fig. 28. Limit analysis results for the defined collapse mechanisms.

WOM model, safety in the +X direction is not verified in the limit analysis result while verified by the pushover result. However, results in the -X direction do not confirm verification in both methods.

6. Conclusions

The objective of this research was the evaluation of the seismic performance of the Soltaniyeh Dome in Iran. The study comprised several phases, including an examination of the geographical location of the building, a comprehensive literature review, a historical survey, and in-situ visual inspections to evaluate existing damage. The subsequent phase involved the preparation of three numerical three-dimensional finite element models to assess the response of the structure under vertical and seismic loading conditions. The first numerical model presents the original configuration of the structure (WM), in the second numerical model minarets were removed (WOM), and the third numerical model presents the current configuration (CC) of the structure. Due to the vast scale of the finite element model and the current propped state of the building, constraints hindered the execution of dynamic identification tests and dynamic structural analysis. On the other hand, stability of the structure was evaluated by means of limit analysis based on macroblocks.

In terms of numerical modeling, the original configuration of the mausoleum (WM) presented a significantly high safety level for vertical loading (5 g). Pushover analyses for the WM and CC models identified minarets as the most vulnerable part of the structure. Moreover, limit analysis for the mechanisms involving the belfry and the whole minaret did not comply with the safety verifications. These results demonstrate that, the main failure of the structure is due to the overturning of the minarets. The partial collapse and the absence of the belfries in the current configuration of the structure also confirms this observation.

Results from the second FE model (WOM), present higher load capacity and consequently notably higher levels of damage compare to the WM model. In this model concentration of damage is on the dome and the tomb. Considering the tomb, results from pushover analysis and limit analysis are in agreement and indicate that the safety of the tomb is not validated. Moreover, result from pushover analysis indicate safety of the dome while the safety of the dome is not confirmed in the results obtained from the limit analysis.

Considering the obtained results, it is important to highlight that, while the mass of the minarets may contribute to the stability of the dome against seismic forces, their susceptibility to collapse poses a significant risk to other parts of the structure noticeably the dome. Therefore, constant monitoring and retrofitting of the minarets are recommended to ensure the structural integrity of the mausoleum. Additionally, the effectiveness of the retrofitting measures implemented on the minarets during the 1970 s require further evaluation.

The research findings underscore the importance of understanding the geometric and structural properties of monuments, as they reflect the harmonious integration of aesthetic and structural elements achieved by master builders. This integration considers not only architectural traditions but also the environmental characteristics of the region.

The research findings offer invaluable insights for selecting restoration and intervention strategies to reduce seismic vulnerability in domed structures. Additionally, they contribute to the development of management strategies, including conservation and maintenance plans, to guide future decisions and prevent unsuitable rehabilitation efforts.

Declaration of Competing Interest

The authors declare that they have no known competing financial interests or personal relationships that could have appeared to influence the work reported in this paper.

Acknowledgments

The work presented in this paper was financed by I.P./MCTES through national funds (PIDDAC) under the R&D Unit of the Institute for Sustainability and Innovation in Structural Engineering (ISISE), at the University of Minho under reference number UIDB/04029/2020-12. The support is gratefully acknowledged.

Also, especial thanks to Saba Ratebi, and Mehdi Ali Verd Beigi for their collaboration in the preparation of the preliminary data.

References

[1] Zomarshidi H. Vaults and Arches in Iranian Architecture (In Persian). 1st ed. Tehran: Omran va behsazi shahri Iran Company; 2008.
[2] Feizolahbeigi A., Lourenço P.B. Study of the Iranian vaults, based on historic aspects, typologies, and geometric rules to reveal the long-term stability reasons. In: 4th International Congress on Luso- Brazilian Construction History. Guimaraes; 2023. p. 549–62.
[3] Reuther O. Sasanian Architecture: in Survey of Persian Art. Vol. 1. 1938. 498 p.
[4] Sanpaolesi P. La cupola di Santa Maria del Fiore ed il mausoleo di Soltanieh. Rapporti di forma e struttura fra la cupola del Duomo di Firenze ed il mausoleo del Ilkhan Ulgiaitu a Soltanieh in Persia. Mitteilungen des Kunsthistorischen Institutes in Florenz [Internet]. 2018 Nov 8 [cited 2023 Apr 14];16(3):221–60. Available from: ⟨https://journals.ub.uni-heidelberg.de/index.php/mkhi/article/view/54269⟩.
[5] Bayraktar A, Hökelekli E, Yang T. Seismic failure behavior of masonry domes under strong ground motions. Eng Fail Anal 2022;142:106749 (Dec).
[6] Varma M, Ghosh S, Milani G. Finite element thrust line analysis of cracked axisymmetric masonry domes reinforced with tension rings. Int J Mason Res Innov 2018;3(1):72.
[7] Scacco J, Grillanda N, Milani G, Lourenço P. Novel non-linear static numerical model for curved masonry structures based on a combined adaptive limit analysis and discrete FE computations. Int J Solids Struct 2022;236–237:111265 (Feb).
[8] Pavlovic M, Reccia E, Cecchi A. A procedure to investigate the collapse behavior of masonry domes: some meaningful cases. Int J Archit Herit 2016;10(1):67–83. Jan 2.
[9] Sharbaf A, Bemanian M, Daneshjoo K, Shakib H. Masonry dome behavior under gravity loads based on the support condition by considering variable curves and thicknesses. Buildings 2021;11(6):241. Jun 4.
[10] Çalık İ, Bayraktar A, Türker T, Karadeniz H. Structural dynamic identification of a damaged and restored masonry vault using Ambient Vibrations. Measurement 2014;55:462–72 (Sep).
[11] Grillanda N, Chiozzi A, Milani G, Tralli A. Collapse behavior of masonry domes under seismic loads: an adaptive NURBS kinematic limit analysis approach. Eng Struct 2019;200:109517 (Dec).
[12] Öztürk Ş, Bayraktar A, Hökelekli E, Ashour A. Nonlinear structural performance of a historical brick masonry inverted dome. Int J Archit Herit 2020;14(8):1161–79. Sep 13.
[13] Nodargi NA, Bisegna P. Minimum thrust and minimum thickness of spherical masonry domes: a semi-analytical approach. Eur J Mech - A/Solids 2021;87: 104222 (May).
[14] Hejazi M, Pourabedin M. Performance of Persian brick masonry discontinuous double-shell domes against earthquakes. Eng Fail Anal 2021;119:104994 (Jan).
[15] Chiorino M, Ceravolo R, Spadafor A, Zanotti Fragonara L, Abbiati G. Dynamic characterization of complex masonry structures: the sanctuary of vicoforte. Int J Archit Herit 2011;5(3):296–314. Apr 11.
[16] Feizolahbeigi A, Lourenço PB, Golabchi M, Ortega J, Rezazadeh M. Discussion of the role of geometry, proportion and construction techniques in the seismic behavior of 16th to 18th century bulbous discontinuous double shell domes in central Iran. J Build Eng 2021;33.
[17] Sallam M, Hassan H, Sayed M, Abdel Hafiez H, Zahra HS, Salem M. Seismic vulnerability assessment of historical minarets in Cairo. Geoenviron Disasters 2023;10(1):30. Dec 11.
[18] Inci P., Halici O.F., Demir C., Comert M., Aldirmaz B., Coban S., et al. Investigation Procedure for the Diagnosis of Historical Minarets: Inclined Minaret of Sivas Ulu Cami (Mosque). In 2024. p. 59–70.
[19] Seker S., Sahin H. Numerical Investigation of a Historic Masonry Minaret Subjected To Seismic Excitation. Iranian Journal of Science and Technology, Transactions of Civil Engineering. 2023 Nov 18;
[20] Nodargi NA, Bisegna P. A new computational framework for the minimum thrust analysis of axisymmetric masonry domes. Eng Struct 2021;234:111962 (May).
[21] Ashcroft IA, Mubashar A. Numerical Approach: Finite Element Analysis. Handbook of Adhesion Technology. Berlin, Heidelberg: Springer Berlin Heidelberg,; 2011. p. 629–60.
[22] Lourenço P, Mendes N, Ramos LF, Oliveira DV. Analysis of masonry structures without box behavior. Int J Archit Herit 2011:369–82.
[23] Simon J, Bagi K. Discrete element analysis of the minimum thickness of oval masonry domes. Int J Archit Herit 2016;10(4):457–75. May 18.
[24] Portioli F, Mammana O, Landolfo R, Mazzolani FM, Krstevska L, Tashkov L, et al. Seismic retrofitting of mustafa pasha mosque in skopje: finite element analysis. J Earthq Eng 2011;15(4):620–39. Apr 7.

[25] Ochsendorf J.A. Collapse of masonry structures. [Cambridge]: University of Cambridge Doctoral Thesis; 2002.
[26] Roca P, Cervera M, Gariup G, Pelà L. Structural analysis of masonry historical constructions. Classical and advanced approaches. Comput Methods Eng 2010;17:299–325.
[27] Huerta S. Galileo was wrong: The geometrical design of masonry arches. Nexus Netw J 2006;8(2):25–51.
[28] Erdogmus E. Timbrel domes of guastavino: nondestructive assessments on a half-scale model. Int J Archit Herit 2008;2(4):330–52. Nov 20.
[29] Aşıkoğlu A, Avşar O, Lourenço PB, Silva LC. Effectiveness of seismic retrofitting of a historical masonry structure: Kütahya Kurşunlu Mosque, Turkey. Bull Earthq Eng 2019;17(6):3365–95. Jun 2.
[30] Destro Bisol G. Safety Assessment of the Shah Mosque in Isfahan, Iran. [Guimaraes]: University of Minho; 2019.
[31] Sorensen A, Erdogmus E. Horizontal support displacement of a thin-tile masonry dome: experiments and analysis. J Perform Constr Facil 2015;29(2) (Apr).
[32] Preciado A, Santos J, Silva C, Ramírez-Gaytán A, Falcon JM. Seismic damage and retrofitting identification in unreinforced masonry Churches and bell towers by the september 19, 2017 (Mw = 7.1) Puebla-Morelos earthquake. Eng Fail Anal 2020;118:104924 (Dec).
[33] Pecorelli ML, Ceravolo R, Epicoco R. An automatic modal identification procedure for the permanent dynamic monitoring of the sanctuary of vicoforte. Int J Archit Herit 2020;14(4):630–44. Apr 20.
[34] Çalik İ, Bayraktar A, Türker T, Akköse M. Empirical formulation for estimating the fundamental frequency of historical stone mosques with masonry domes. Struct Des Tall Spec Build 2020;29(9). Jun 25.
[35] Ceravolo R, De Marinis A, Pecorelli ML, Zanotti Fragonara L. Monitoring of masonry historical constructions: 10 years of static monitoring of the world's largest oval dome. Struct Control Health Monit 2017;24(10):e1988 (Oct).
[36] Birel A., Koçak B., Bayrak O.F., Durgut E., Ispir M., Ilki A. Planning the Shaking Table Tests of a Historical Brick Minaret Representing Mid-Height Early Ottoman Period Architecture. In 2024. p. 71–83.
[37] Jurina L. Reinforced Arch Method" in the consolidation of masonry arches and vaults: Experimental results. In: Brick and Block Masonry. 1st ed. CRC Press; 2016. p. 8.
[38] Mora Alonso-Muñoyerro S, Rueda Marquez de la Plata A, Cruz Franco P. Consolidation of Historical Masonry: Past Experiences and Future Forecast. Construction and Building Research. Dordrecht: Springer Netherlands,; 2014. p. 299–303.
[39] Lourenco P.B., Gaetani A. Influences and analogies between masonry arch and cross vault: from construction to seismic response.
[40] Cusano C, Montanino A, Cennamo C, Zuccaro G, Angelillo M. Geometry and stability of a double-shell dome in four building phases: the case study of Santa Maria Alla Sanità in Naples. Int J Archit Herit 2023;17(2):362–88. Feb 1.
[41] Huerta Fernandez S., Aroca Hernandez-Ros R. Masonry domes: a study on proportion and similarity.
[42] Novello G., Piumatti P. Geometrical analysis of the largest oval dome in the world. 2012;
[43] Hejazi M. Seismic vulnerability of Iranian historical domes. Trans Built Environ 2003;72.
[44] Vasseghi A, Eshghi S, Jabbarzadeh MJ. Preliminary seismic evaluation of the historic Sultaniyeh Dome. JSEE 2007;8(4).
[45] Ghaemi S., Bakhshi A. Seismic evaluation and rehabilitation of the historic building, a case study about Soltaniyeh dome. [Tehran]: Sharif University of Technology; 2013.
[46] Kalantari H, Nasserasadi K, Arjmandi A. Seismic vulnerability study of Soltaniyeh dome using nonlinear static and dynamic analyses. Int J Adv Struct Eng 2018;10:367–80 (Sep).
[47] Betti M, Bonora V, Galano L, Pellis E, Tucci G, Vignoli A. An Integrated Geometric and Material Survey for the Conservation of Heritage Masonry Structures. Heritage 2021;4(2):585–611.
[48] Mendes N. Masonry macro-block analysis [Internet]. Guimaraes: University of Minho; Available from: ⟨https://repositorium.sdum.uminho.pt/handle/1822/39038⟩.
[49] Portioli F., Casapulla C., Cascini L., D'Aniello M., Landolfo R. Limit analysis by linear programming of 3D masonry structures with associative friction laws and torsion interaction effects. Archive of Applied Mechanics [Internet]. 2013 Oct 23 [cited 2023 Nov 13];83(10):1415–38. Available from: ⟨https://link.springer.com/article/10.1007/s00419–013-0755–4⟩.
[50] Gilbert M, Casapulla C, Ahmed HM. Limit analysis of masonry block structures with non-associative frictional joints using linear programming. Comput Struct 2006;84(13–14):873–87. May 1.
[51] Orduna A, Lourenço PB. Three-dimensional limit analysis of rigid blocks assemblages. Part II: Load-path following solution procedure and validation. Int J Solids Struct 2005;42(18–19):5161–80. Sep 1.
[52] Kamenjarzh J., Jacov A. CRC Press. 1996 [cited 2023 Nov 13]. Limit Analysis of Solids. Available from: ⟨https://www.amazon.com/Limit-Analysis-Solids-Structures-Kamenjarzh/dp/084932873X⟩.
[53] Kooharian A. Limit analysis of Voussoir (Segmental) and concrete archs. J Proc 1952;49(12):317–28. Dec 1.
[54] Nodargi N, Bisegna P. Collapse capacity of masonry domes under horizontal loads: A static limit analysis approach. Int J Mech Sci 2021;212:106827 (Dec).
[55] Milani G, Bucchi A. Kinematic FE homogenized limit analysis model for masonry curved structures strengthened by near surface mounted FRP bars. Compos Struct 2010;93(1):239–58 (Dec).
[56] Nodargi N, Bisegna P. A finite difference method for the static limit analysis of masonry domes under seismic loads. Meccanica 2022;57(1):121–41. Jan 23.
[57] Ventura G, Coppola M, Calderini C, Chiorino MA. Three-Dimensional Limit Analysis of the Vicoforte Elliptical Dome. Int J Archit Herit 2014;5(8):649–69. Sep 3.
[58] Heyman J. The stone skeleton. Int J Solids Struct 1996;2(2):249–79.
[59] Funari M.F., Mehrotra A., Lourenço P.B. A Tool for the Rapid Seismic Assessment of Historic Masonry Structures Based on Limit Analysis Optimisation and Rocking Dynamics. Applied Sciences 2021, Vol 11, Page 942 [Internet]. 2021 Jan 21 [cited 2023 Nov 13];11(3):942. Available from: ⟨https://www.mdpi.com/2076–3417/11/3/942/htm⟩.
[60] Cultural Heritage Organization of Iran. The dome of soltaniyeh the pasture which became the capital city of an empire. 2005.
[61] Schroeder E., Pope A.U., Ackerman P. A Survey of Persian Art: The Seljūq Period. Vol. III. Tokyo: Oxford; 1967.
[62] Fletcher B. A History of Architecture on the Comparative Method [Internet]. 2023 [cited 2023 Apr 15]. Available from: ⟨https://www.amazon.com/History-Architecture-Comparative-Method-17th/dp/B0007J9NCK⟩.
[63] A Short Account of Early Muslim Architecture: K. A. C. Creswell: Amazon.com: Books [Internet]. [cited 2023 Apr 15]. Available from: ⟨https://www.amazon.com/Short-Account-Early-Muslim-Architecture/dp/B000NTZDFA⟩.
[64] Iranian Cultural Heritage Documentation Center.
[65] Irani A. Structural Assessment and Historical Review of the Dome at Soltaniyeh. Massachusetts Institute of Technology,; 2015.
[66] Memarian GH. Persian architecture: Construction. Tehran: Naghme Nowandish,; 2012.
[67] Kasaee R., Sanpaulesi P. Restoration project of mausoleum of Oljaito in Soltaniyeh. Tehran; 1968.
[68] Mojabi M. Restoration report of Soltaniyeh Doma. Tehran; 1980.
[69] Francesco Pisani. Il Mausoleo di Oljeitu a Soltaniyeh. I restauri di Piero Sanpaolesi a quindici anni dall'iscrizione nella lista del patrimonio mondiale dell'UNESCO. Restauro Archeologico, Journal of the Department of Architecture University of Florence. 2020;
[70] National building constitution organization of Iran. Design Loads for Buildings (Code 6). Tehran: Toosee; 2013.
[71] Cen, EN 1998–3 Euro Code 8: Design of Structures for Earthquake Resistance– Part 3: Strengthening and Repair of Buildings. 2005.
[72] Iranian Code of Practice for Seismic Resistant Design of Buildings, Standard No. 2800. Vol. 4. Tehran: Iranian Road, Housing and Urban Development Research Center; 2013. p. 152.
[73] Georgiou A, Kotakis S, Loukidis D, Ioannou I. Case study of seismic assessment of a short irregular historic reinforced concrete structure: time-history vs. pushover nonlinear methods. J Earthq Eng 2023;27(16):4761–85. Dec 10.
[74] Benavent-Climent A, Escolano-Margarit D. Shaking table tests of structures with hysteretic dampers: experimental results versus prediction using non-linear static methods. Bull Earthq Eng 2012;10(6):1857–83. Dec 24.
[75] Mahdi T, Soltangharaei V. Plan irregular RC frames: comparison of pushover with nonlinear dynamic analysis. Asian J Civ Eng 2011;12(6):679–90. Dec;12(6):679–690.
[76] Bhatt C, Bento R. The extended adaptive capacity spectrum method for the seismic assessment of plan-asymmetric buildings. Earthq Spectra 2014;30(2):683–703. May 8.
[77] Bektas N, Kegyes-Brassai O. Conventional RVS methods for seismic risk assessment for estimating the current situation of existing buildings: a state-of-the-art review. Sustainability 2022;14.
[78] Degli Abbati S, D'Altri AM, Ottonelli D, Castellazzi G, Cattari S, de Miranda S, et al. Seismic assessment of interacting structural units in complex historic masonry constructions by nonlinear static analyses. Comput Struct 2019;213:51–71. Mar 1.
[79] Zameeruddin M, Sangle KK. Performance-based seismic assessment of reinforced concrete moment resisting frame. Eng Sci 2021;33:153–6.
[80] Kalkan E, Kunnath SK. Assessment of current nonlinear static procedures for seismic evaluation of buildings. Eng Struct 2007;29:305–16.
[81] Máca J., Oliveira D.V. Seismic behaviour and structural dynamics. SAHC slides SA3. Guimarães; 2018.
[82] Huan H, Sander JHM. Verif Mater Models Mason walls Nonlinear pushover Anal 2023:3994–4003.
[83] Argiento LU, Mousavian E, Casapulla C, Ceroni F. Pushover analysis of rocking façades in masonry churches: the role of friction and geometry in identifying homogeneous classes of vulnerability. Procedia Struct Integr 2023;44:1388–95.
[84] Beconcini ML, Formichi P, Giresini L, Landi F, Puccini B, Croce P. Modeling approaches for the assessment of seismic vulnerability of masonry structures: the E-PUSH program. Buildings 2022;12(3):346. Mar 12.
[85] Alejo L., Mendes N., Lourenco P. The effect of morphology on the structural behaviour of masonry walls. In: Congreso de Métodos Numéricos en Ingeniería. 2017.
[86] NTC Norme Tecniche per le Costruzioni. D.M. del ministero delle infrastrutture e dei trasporti; 2018.
[87] Pre-Standard and Commentary for the Seismic Rehabilitation of Buildings. Federal Emergency Management Agency USA; 2000.
[88] American Society of Civil Engineers and Structural Engineering Institute. Seismic Evaluation and Retrofit of Existing Buildings: ASCE/SEI. American Society of Civil Engineers and Structural Engineering Institute USA; 2017.

[89] Applied Technology Council. Seismic Evaluation and Retrofit of Concrete Buildings. Applied Technology Council Proposition USA; 1996.

[90] New integrated knowledge-based approaches to the protection of cultural heritage from earthquake-induced risk. Padova: Università di Padova; 2010.

[91] Feizolahbeigi, A. Golabchi, M. and Reza-Zadeh, M. "An investigation in Geometry and Proportion in relation with Structural System in Buildings with Discontinuous Double Shell Domes in Tafresh Region," *Soffeh*, vol. 31, no. 3, pp. 21–42, Sep. 2021, doi: 10.52547/SOFEH.31.3.21.